VIP blockade leads to microcephaly in mice via disruption of Mcph1-Chk1 signaling

Sandrine Passemard, Vincent El Ghouzzi, Hala Nasser, Catherine Verney, Guilan Vodjdani, Adrien Lacaud, Sophie Lebon, Marc Laburthe, Patrick Robberecht, Jeannette Nardelli, et al.

VIP blockade disrupts Mcph1-Chk1 signaling leading to microcephaly in mice

Sandrine Passemard [1-4], Vincent El Ghouzzi [1,2], Hala Nasser [1,2], Catherine Verney [1,2], Guilan Vodjdani [5], Adrien Lacaud [6,7], Sophie Lebon [1,2], Marc Laburthe [2,8], Patrick Robberecht [9], Jeannette Nardelli [1,2], Shyamala Mani [10], Alain Verloes [1,2,4], Pierre Gressens [1-3,11]* and Vincent Lelièvre [1,2,6,7]*

1. Inserm, U676, Paris, France
2. Université Paris 7, Faculté de Médecine Denis Diderot, Paris, France
3. AP HP, Hôpital Robert Debré, Service de Neurologie Pédiatrique, Paris, France
4. AP HP, Hôpital Robert Debré, Service de Génétique Clinique, Paris, France
5. Centre de Recherche de l'Institut du Cerveau et de la Moelle épinière, CNRS UMR-7225, Inserm UMR-975, Université Pierre et Marie Curie, Paris, France
6. CNRS, UPR 3212, Strasbourg, France
7. Université de Strasbourg, Strasbourg, France
8. Inserm, U773, Paris, France
9. Laboratory of Biological Chemistry and Nutrition, ULB, Brussels, Belgium
10. Center for Neuroscience, IISc, Bangalore, India
11. Institute for Reproductive and Developmental Biology, Imperial College, Hammersmith Campus, London, UK

*These authors have equally contributed to the manuscript

Address for correspondence

Dr Pierre Gressens

Inserm U676, Hôpital Robert Debré, 48 blvd Serurier, F-75019 Paris, France

Phone : +33 1 40 03 19 76; Fax : +33 1 40 03 19 95; pierre.gressens@inserm.fr

or

Dr Vincent Lelièvre

CNRS UPR-3212, 5 rue Blaise Pascal, F-67084 Strasbourg Cedex, France

Phone : +33 3 88 45 66 59; Fax : +33 3 88 60 16 64; lelievre@inci-cnrs.unistra.fr

Conflict of interest statement

The authors have declared that no conflict of interest exists

ABSTRACT

Human Primary Microcephaly is a genetic disorder that elicits a reduction of cortical outgrowth without severe interference with cortical patterning. It has been associated with mutations in *MCPH1, WDR62, CDK5RAP2, CEP152, ASPM, CENPJ,* and *STIL* genes. These genes are involved in mitotic spindle formation and centrosomal activities or in control of cell cycle. We have shown previously that blocking the vasoactive intestinal peptide (VIP) using a VIP antagonist (VA) during murine gestation results in microcephaly. Using this model, we show that the cortical abnormalities mimic the phenotype described in MCPH patients and that VIP blockade during neurogenesis specifically disrupts Mcph1 signaling. VA induced selective alterations of *Mcph1* expression and function. Inhibition of *Mcph1* expression preceded the down-regulation of *Chk1* expression and the reduction of Chk1 kinase activity. This inhibition of *Mcph1* and *Chk1* affected the expression of a specific subset of cell cycle-controlling genes and turned off neural stem cell proliferation in neurospheres. Furthermore in vitro silencing of *Mcph1 or Chk1* in neurospheres mimicked the VA-induced inhibition of cell proliferation. These results demonstrate that VIP blockade induces microcephaly through Mcph1 signaling and suggest that VIP/Mcph1/Chk1 signaling is key for normal cortical development.

INTRODUCTION

Microcephaly Primary Hereditary (MCPH) is a genetic affection often characterized by a severe reduction of brain size without cortical cyto-architecture defect, as defined at birth by an Occipital Frontal Circumference (OFC) below -2 SD or more from normal range (1). MCPH patients usually exhibit mild developmental delay associated with hyperkinesia and, most often, mild to severe cognitive impairment (2, 3). Seven genes are currently identified in MCPH-related patients, namely *BRIT1/MCPH1* (BRCT-Repeat Inhibitor of hTert expression, that encodes MICROCEPHALIN; locus MCPH1) (4), *WDR62* (WD repeat domain 62; MCPH2) (5-7), *CDK5RAP2 (*Cyclin Dependent-Kinase 5 Regulatory Associated Protein 2*;* MCPH3) (8), *CEP152* (centrosomal protein 152 kDa; MCPH4) (9), *ASPM* (Abnormal Spindle-like Microcephaly Associated Protein; MCPH5) (10), *CENPJ (*Centromeric Protein J*;* MCPH6) (8) and more recently *STIL/SIL (*SCL/TAL1 interrupting locus*;* MCPH7) (11). While mutation-induced loss of function triggers a reduction of cortical expansion in MCPH-related patients, native proteins were found involved in cell cycle/checkpoint control (*MCPH1* and *STIL,* (12-15)), and/or mitotic spindle dynamics (*MCPH1*, *WDR62, CDK5RAP2, CEP152, ASPM, CENPJ and STIL* (8, 16-18)). In addition, *MCPH1, CEP152* and *STIL* were also implicated in radiation-induced DNA repair, apoptosis or cancer (12, 19-25). Downstream, *CHK1,* a target for *MCPH1*, is known to control progression of the cell cycle at crucial phases including S phase and G2/M transition (14, 15, 21, 22, 25).

Although animal models would be of great help to better understand MCPH-linked mechanisms, very few of them, displaying MCPH phenotype, are available so far. Genetic invalidations of intrinsic factors (i.e. *Stil, Chk1, Brca1*) have been carried out in mice but resulted in lethal phenotypes in utero (19, 26, 27). Two *Mcph1* knockout mice were very recently described (28, 29). In the *Mcph1/Brit1* conditional invalidation driven by the *β-actin* promoter, mutant mice exhibit mitotic and meiotic recombination, DNA repair defects

resulting in genomic instability and infertility (28). However, the brain phenotype has not yet been reported. In the other model, which was generated by gene trapping leading to the deletion of the C-terminal BRCT domain of Mcph1, adult mice do not have detectable brain weight loss although no detailed neuropathology has been reported (29). In addition, about 1,200 genes were either up-regulated or down-regulated when compared to WT brain (29). Interestingly, the *Nde1*$^{-/-}$ mouse (*NUDE* in humans, encoding a microtubule organizing center (MTOC) associated protein) is the only published genetic mouse model with a developmental brain phenotype showing a significant reduction (around 20%) of the overall brain volume with a specific reduction of upper layers (30). However, loss of function of NUDE has not been reported in MCPH-related patients.

Developmental processes that are controlled by the MCPH loci may also depend on environmental factors. Deleterious extrinsic factors including alcohol, caffeine, morphine or chemotherapeutic agent have been shown to modulate cell cycle duration and symmetrical vs. asymmetrical divisions to limit the number of newborn cortical neurons (31-35). However, specific molecular targets of these extrinsic factors are not yet elucidated, except for ionizing radiation shown to negatively impact the brain development by interfering with the ATR/CHK1/PCNT pathway (36). Conversely, beneficial extrinsic factors either produced by the embryo (including IGF-I and FGF10), or that cross the placenta barrier when produced by the mother (i.e. vitamin D3, thyroid hormone T3, NT3 or serotonin), can sustain boost or modulate the embryonic brain development (37-40). Among these maternal factors, the vasoactive intestinal polypeptide (VIP) is produced in great amount during pregnancy (41) by lymphocytes present in decidual membranes (42) and elicits various neurotrophic actions including a major growth factor effect on embryogenesis as shown previously on whole embryos treated *ex utero* with VIP (43). To date, none of these extracellular factors have been

clearly connected with this ubiquitous machinery that dictates the appropriate number of neurons necessary to ensure the normal brain functions.

In line with these data, in the early 90's, Gressens and co-workers have described a pharmacologically-induced murine model of microcephaly (44). In the latter, maternal VIP was challenged by a well characterized VIP synthetic antagonist (VA) (45-47) which, when injected to pregnant females during neurogenesis (E9-11) led to cortical alterations of newborn pups. These alterations involve the size but not the architecture of the cortex, a phenotype reminiscent of MCPH features in humans. Follow-up studies by the same investigators have suggested that VIP action on embryonic cortical expansion was related to a reduction of cell cycle duration including a shortening of the S phase (48). Nevertheless, at that time, no molecular mechanism was offered to explain such a drastic phenotype.

In the present study, we used this animal model and sought after the possible mechanism by which extrinsic factors such as VIP control cell cycle duration. To address this issue, we aimed to correlate VA-induced alteration of VIP signaling pathway with modulation of expression of MCPH genes and their functions both in vivo and in vitro using embryos, newborn mice and neurosphere-derived progenitors. We demonstrate that VIP blockade specifically down-regulates *Mcph1-Chk1* expression and function, ultimately leading to cortical abnormalities that closely mimic features described in MCPH patients.

RESULTS

VIP blockade during neurogenesis induces microcephaly with thinner cortex

VIP blockade results in microcephaly in mice: however, the phenotype has not been described yet at the histological and morphometric levels. A global morphometric analysis of brains from P5 pups born from either VA- or PBS-injected dams was performed. VA brains showed a reduced weight as compared to controls at P5 and P10, without statistically significant body weight reduction (supplemental Figure 1A-B). On Nissl stained sections, a clear qualitative shrinkage of cortical thickness was observed (supplemental Figure 1C-D).

On selected coronal rostral and caudal levels of the primary somatosensory cortex (S1) (see supplemental methods), cortical surface (supplemental Figure 1E) and thickness (supplemental Figure 1F) were decreased in VA-treated animals as compared to controls. The cortical layers were thinner in VA than in controls, but differences were slightly bigger in rostral than in caudal somatosensory areas (i.e. 19%: 789+/-92µm *vs.* 645+/-68µm and 17%: 974+/-63µm *vs.* 775+/-55µm, respectively, n= per condition) (supplemental Figure 1G).

The cortical neuronal density, assessed at the rostral level in the primary somatosensory cortex, did not reveal any significant difference in the number of neuronal nuclei (NeuN)-labeled neurons per surface unit between VA and controls (8180+/-1085cells/μm^2, n=3; control, 8780+/-778cells/μm_2, n=4) (supplemental Figure 1H). However, measurement of the thickness of the superficial cortical layers (II-III-IV) versus deeper layers (V-VI) revealed a reduction of both upper and deeper layers thickness (supplemental Figure 1G-H). The use of specific markers of cortical layers (Cux1, expressed in layers II-IV, Satb2, expressed by a subset of neurons throughout the cortical layers with a most prominent expression in layers II-IV, and Tbr1, expressed in layer VI) confirmed that all layers were affected by VA treatment (Figure 1). Astrocytes distribution appeared unchanged between groups as revealed by GFAP immunodetection (data not shown).

Taken together, these data suggest that VIP blockade during early neurogenesis has a dramatic impact on cortical development.

VIP blockade decreases proliferation in neuroepithelial progenitors by increasing cell cycle length

To address whether VA could directly impact neurogenesis, we analyzed proliferation and cell cycle length in embryos. Since the thickness reduction was already detectable as early as E12.5 in lateral telencephalic wall of VA-treated embryos (Figure 2A-B), we analyzed progenitors proliferation one day before, i.e. in E11.5 VA-treated embryos and controls. To assess a potential decrease in cell proliferation, we first measured the cell cycle length in VA-treated and control telencephalic samples, using an elegant method previously described (49). Iododeoxyuridin (IdU) was injected into E11.5 pregnant females followed by BrdU (50mg/g body weight ea. for both) 1,5h later. Dams were sacrificed 2h after the first injection (Figure 2D). As observed in Figure 2C and Supplemental Table 1, both BrdU and IdU labeling were reduced in VA animals. Cell cycle length calculation shown on Figure 2E was performed by extracting the following parameters S phase (Ts), Total cycle (Tc) durations as well as the Ts/Tc ratio, from the number of positive cells for BrdU, IdU or both. In line with previous studies (50, 51) performed in E11.5 ventricular zone (VZ) control brains, Ts was ~ 5,4h and Tc ~ 12h. In VA treated brains, both Ts and Tc were significantly lengthened: Ts ~ 8,5h and Tc ~ 29h, confirming that VA-induced VIP blockade between E9-E11 reduces VZ progenitor proliferation by increasing the duration of both the S phase and the whole cell cycle.

At this stage, the number of apoptotic cells (cleaved caspase-3 and TUNEL positive) in the dorsal ventricular zone was similar in VA and control telencephalon (Figure 2F and data not shown).

VIP blockade accelerates cell cycle exit and leads to early differentiation of cortical progenitors

Since the reduction of VZ progenitors appeared secondary to the cell cycle lengthening in VA-treated telencephalon, we aimed to characterize the cell fate of these progenitors. Therefore, we studied at E11.5 the expression pattern of p27kip1, a factor known to promote cell cycle exit of cortical progenitors (52). P27kip1 positive cells were highly increased in dorsal telencephalon of VA-treated embryos as compared to age-matched controls, indicating that VIP blockade during early neurogenesis significantly promotes VZ progenitors to exit the cell cycle (Figure 3A-B).

To investigate whether this loss of progenitors could influence the normal cell differentiation during early neurogenesis and corticogenesis phases, we assessed the doublecortin (DCX) immunoreactivity in telencephalon of E12 control and VA-treated embryos. DCX is a microtubule-associated protein whose expression underlines mitosis exit and is commonly used as an early marker of newborn post mitotic neurons (53). DCX was expressed in VA treated cortices with highest signals in lateral ganglionic eminence (LGE), while it remained undetectable in control cortices at this stage (Figure 3C). Similarly, immunostaining at E11.5 for Calretinin, a marker for Cajal Retzius neurons was not visible in controls while it strongly labeled VA-treated cortices (Figure 3D). Interestingly, DCX- and Calretinin-positive post-mitotic neurons were predominantly detected in the dorsal, lateral and medial preplate and in LGE from VA-treated cortices (Figures 3C-D).

Together, our results indicate that VIP blockade during early neurogenesis promotes cell cycle exit and premature neuronal differentiation of VZ progenitors in both dorsal and ventral telencephalon without increased apoptosis.

VIP blockade inhibits the neurotrophic VIP signaling through cAMP-coupled VPAC receptors

To further dissect VIP signaling in our model, we first asked whether VIP receptors are expressed during neurogenesis. To this end, we measured the level of expression of the three known VIP and PACAP receptors (*Vpac1, Vpac2* and *Pac1*) by quantitative PCR using RNA extracts from E12 and E16 embryonic forebrains and neurosphere-derived progenitors isolated from E10.5 forebrains. VIP and PACAP may actually interact with all three receptors although VPAC2 and PAC1 are the predominant forms at these early stages of brain development. As shown in Figure 4A, *Vpac1, Vpac2* and *Pac1* were expressed in neural stem cells as well as E12 and E16 telencephalon.

To dissect VIP signaling pathway during the intense proliferative period of neural progenitors, we studied proliferation of neurospheres-derived progenitors with a BrdU incorporation assay (see Methods) in the presence of VIP, VIP agonists, VA and activators or inhibitors of cAMP-PKA pathway. As shown in Figure 4 B-C, VIP stimulated in a dose-dependant and with a classical bell-shaped curve (54) the proliferation of progenitors and its maximal effect on BrdU incorporation was completely abolished in the presence of VA. VA alone reduced BrdU incorporation (Figure 4D). The proliferative effect of VIP at nanomolar concentration that excluded an effect through PAC1 receptor by definition (55) could be mimicked by both VPAC1 (Figure 4E-F) and VPAC2 agonists (Figure 4G). Finally, VIP stimulatory effect was completely abolished by two different PKA inhibitors (H89 and KT5920) and mimicked by forskolin (FSK), an adenylate cyclase activator (Figure 4H). All together these data suggest that VIP-induced proliferative actions are mediated by VPAC receptors positively coupled with a cAMP/PKA signaling pathway and that this pathway is blocked by VA.

VIP blockade leads to in vivo inhibition of *Mcph1* expression

To explore a putative crosstalk between VIP signaling and *MCPH*-related genes, we analyzed *Mcph* genes expression in telencephalon of both VA-treated-animals and controls at different stages. RNA samples were extracted from telencephalon of control and VA-treated embryos between E12 and P0. Quantitative RT-PCR experiments were performed to measure the expression levels of different genes known to be relevant in human microcephaly, namely *MCPH1*, *WDR62*, *CDK5RAP2*, *CEP152, ASPM* (commonest cause of MCPH), *CENPJ*, and *STIL*. All of these genes showed a similar ontogenic pattern with a very high expression during neurogenesis and then decreased until birth. However, only *Mcph1* displayed a significant down-regulation in telencephalon of VA-treated embryos at each peaking times (between E12 and P0) as compared to controls (Figure 5 A-G). Moreover, this specific effect of VA on *Mcph1* expression was also observed at the protein level as shown by western blot (supplemental Figure 2). To further assess the specificity of VA on *Mcph1* and its downstream targets, we carried out similar experiments on E16 embryos after treatment with VIP, VA or both between E9 and E11 (Figure 5H-I). While VA reduced the basal level of expression of *Mcph1*, as expected, VIP had opposite effects. Interestingly, VIP was able to rescue the VA-induced inhibition of *Mcph1* (Figure 5H), while *Aspm*, used as a negative control, remained unchanged (Figure 5I). In situ hybridization performed at E12.5 showed that, in control embryos, *Mcph1* was expressed along the whole telencephalon in almost all cells of the neuroepithelium (supplemental Figure 3). In contrast, in VA-treated embryos, *Mcph1* expression was restricted to the outer part of the neuroepithelium of the rostral telencephalon (supplemental Figure 3). Taken together, these data demonstrate that VIP blockade during neurogenesis specifically reduces the expression of *Mcph1* in embryo telencephalon.

VA acts through VPAC1 receptors to block *Mcph1* expression in neurosphere-derived progenitors

To further decipher the signaling pathway triggered by the VIP in our model, we used an in vitro approach based on neurosphere-derived progenitors. As observed in vivo, VA reduced *Mcph1* expression, VIP stimulated *Mcph1* expression, and this latter effect was blocked by co-treatment with VA (Figure 6). VPAC1 agonist but not VPAC2 agonist mimicked VIP-induced expression of *Mcph1* (Figure 6A) and had no effect on *Aspm* expression (Figure 6B). This suggests that, in the same way as in the in vivo experiments, VA specifically inhibits *Mcph1* through VPAC1 signaling in neurosphere-derived progenitors. In vitro, addition of H89 or KT5720 also resulted in significant reduction in expression levels of *Mcph1*, confirming the involvement of PKA activity in the regulation process (Figure 6C). Again, no effect was observed on *Aspm* expression (Figure 6D).

The effect of VIP on proliferation of neurosphere-derived progenitors is abolished in the absence of Mcph1

To confirm the specificity of VIP effects on *Mcph1* signaling, we next aimed to silence *Mcph1* in neurosphere-derived progenitors. Cells were transduced with lentiviral vectors expressing shRNAs, which, once converted into siRNAs, are specifically targeting *Mcph1* mRNA. The expression level of *Mcph1* was analyzed by quantitative PCR and western blot. Data revealed a significant inhibition of *Mcph1* expression by two separate *Mcph1*-targeting shRNAs (Figure 7A). This selective down-regulation of *Mcph1* failed to trigger any effect on *Aspm,* used as a negative control (Figure 7B). Importantly, stimulation of cell growth by VIP was abolished by the selective *Mcph1*-targeting shRNAs (Figure 7C) suggesting that *Mcph1* is required to mediate the effects of VIP on neurogenesis.

VA inhibits *Mcph1-Chk1* signaling both in vivo and in vitro

It has been shown that *MCPH1* regulates *CHK1* and *BRCA1* expression (14, 15). *CHK1* and *BRCA1* are involved in DNA repair and cell cycle check points control (56-59) and also play a role in proliferation of undamaged cells (22, 25, 56, 60-62). However, their roles in neurogenesis have not been investigated.

Before addressing the impact of VIP and VA on the expression of *Chk1* and *Brca1*, we confirmed that in neurosphere-derived progenitors *Mcph1* regulates *Chk1* and *Brca1* expression, using *Mcph1*-targeting shRNAs (supplemental Figure 4).

To determine if *Mcph1* targets are regulated by VIP, we studied *Chk1* and *Brca1* expression in telencephalon of VA-treated embryos and in neurosphere-derived progenitors, by quantitative PCR and western blot. Expression of *Chk1* and *Brca1* genes was found to be decreased by in vivo VA treatment (Figure 8A-B). Western blot analysis of VA-treated embryos confirmed the significant reduction of Chk1 and showed a similar trend for Brca1 (supplemental Figure 5). VIP increased in vivo *Chk1* and *Brca1* expression and was able to rescue VA-induced inhibition of *Chk1* and *Brca1* (Figure 8C-D). In line with the in vivo data, VIP significantly increased *Chk1* expression in neurosphere-derived progenitors (Figure 8E). Its effects on *Chk1* expression were mimicked by a VPAC1 agonist but not by a VPAC2 agonist (Figure 8E). VA inhibited *Chk1* expression and this effect was mimicked by H89 (Figure 8G). Although it did not reach significance, there was a trend towards an increased expression of *Brca1* following VIP treatment of neurosphere-derived progenitors (Figure 8H). VA significantly inhibited *Brca1* expression and this effect was mimicked by H89 (Figure 8H). Together, these data indicate that VA inhibits *Mcph1-Chk1-Brca1* signaling both in vivo and in vitro trough VPAC1/PKA signaling pathway.

Chk1 is required for VIP proliferative effects on neurosphere-derived progenitors

To assess whether *Chk1* is also necessary to mediate the effect of VIP, we knocked-down the expression of *Chk1* in neurospheres. Neurospheres were transduced with lentiviral vectors expressing various shRNAs, which, once converted into siRNAs, are specifically targeting *Chk1* mRNA. *Chk1* down-regulation was checked by quantitative PCR and western blot (Figures 9A-B) and showed that, out of four different vectors, only the shRNA4 lentiviral vector failed to inhibit *Chk1* expression. BrdU incorporation experiments were carried out to evaluate VIP effects on neurospheres proliferation (Figure 9C) in the lentiviral-transduced cells. As shown in Figure 9C, VIP failed to stimulate proliferation in *Chk1*-ShRNA1- and *Chk1*-ShRNA2-transduced cells but was still able to induce that of cells containing the control sequence or *Chk1*-shRNA4 (used here as a negative control). These data indicate that *Chk1* is required for VIP mitotic effects on neurosphere-derived progenitors proliferation.

VIP blockade interferes with cell cycle by modulating Chk1 functions

To determine whether VA affects Chk1 function in addition to *Chk1* expression, we assessed Chk1 kinase activity in vivo (in forebrain/telecephalon from Control, VIP and VA-treated embryos between E12 to P0) and in vitro (in neurosphere-derived progenitors treated by PBS, VIP or VIP+VA). At each stage in vivo (Figure 10A) and in neurosphere-derived progenitors (Figure 10B) Chk1 kinase activity was strongly reduced in the presence of VA, and strongly enhanced upon VIP stimulation. As expected, H89 blocked VIP effect, thus mimicking VA action, while FSK mirrored VIP activity in vitro (Figure 10B). These data indicate that VIP blockade affects Chk1 function most likely by modulating the cAMP/PKA pathway.

To test whether key checkpoints of cell cycle known to be targets of *Chk1,* were also affected in our model, we analyzed the expression of *Cdc25, Cyclin B* and *Cdk1* (involved in regulation of G2/M transition) and *Cyclin A* and *Cdk2* (regulation of S phase) by quantitative PCR. As shown in Figure 10C-E, VA treatment resulted in a strong decrease of *Cdc25, Cyclin*

B and *Cdk1* expression in vivo. The in vitro approach accordingly showed that VA completely abolishes the effects of VIP on the expression of these genes (Figure 10F-H). By contrast, expression of *Cdk2* and *Cyclin A* remained unchanged both in vivo and in vitro (data not shown). These data indicate that VIP blockade affects specific cell cycle checkpoints and suggest that VIP blockade impacts on the G2/M transition.

To test whether this effect was mediated by Chk1, we analyzed the expression of these G2/M transition checkpoints following down-regulation of *Chk1* expression through the lentiviral-mediated RNA interference approach using the shRNAs specifically directed against *Chk1*. Down-regulation of *Chk1* resulted in a reduced expression of *Cdc25, Cyclin B* and *Cdk1* expression, indicating that the effect observed upon VA treatment is mediated by *Chk1* (Figure 10I-K).

Taken together, these data indicate that VIP blockade interferes with the cell cycle by affecting Chk1 activity and the subsequent modulation of targets involved in G2/M transition.

DISCUSSION

The basis of the high degree of encephalization in humans is not understood. Discovery of the microcephaly locus was an important step in this process as it offered an insight into a set of loci that controlled cortical size without an adverse effect on cortical patterning. Interestingly, evolutionary studies do not seem to support the hypothesis that these loci then must have been positively selected for during vertebrate evolution. In this context there are several external factors that also lead to a large variation in cortical size. Therefore one possible reason for a lack of evidence for the strong positive selection in the MCPH loci is that the high degree of encephalization during evolution is the result of a combination of environmental factors that modulate these genetic loci and therefore the genetic loci itself is but only half the story. To date there has been no evidence linking environmental factors to genes that have been shown to play a role in regulating cortical size and this has remained a speculation. In this study for the first time we show that a maternal factor, VIP, modulates MCPH genetic loci that have been associated with cortical expansion and thus points to a mechanism by which a combination of genetic selection and maternal factors may play a role in regulating cortical size.

The most salient feature of the present study is the demonstration that, in mice, VIP-blockade-induced microcephaly involves *Mcph1* down-regulation, linking a maternal factor to the molecular machinery, which controls the proliferation of neural cell precursors. In addition, in this model, interfering with the expression and/or function of *Chk1*, a known target of *Mcph1*, appears as a key mechanism for the VA-induced blockade of cell cycle. Finally, VIP blockade slows down proliferation of VZ progenitors through lengthening of cell cycle duration and accelerating cell cycle exit and progenitor differentiation.

Is the VA-induced microcephaly a relevant model for human MCPH?

Several lines of evidence support that the present model mimics different key aspects of human MCPH. Indeed, blockade of VIP signaling during neurogenesis induces a reduction in brain weight, in cortical thickness, and in cortical surface, these anomalies being reminiscent of the cortical phenotype observed in patients with MCPH. In addition, VIP blockade induces the inhibition of the *Mcph1* gene expression, one of the seven known genes implicated in MCPH. In contrast, the expression of the other known *Mcph* genes is not affected by VA, supporting the specificity of the effects. Therefore, we believe that the VA model is the first relevant for Mcph1-related human microcephalies.

How does VIP regulate *Mcph1* expression?

Pharmacological and mRNA expression data support the hypothesis that VA effects in cell cycle and brain growth are mediated through VPAC1 receptors expressed on NSC progenitors. In agreement with this hypothesis, VPAC1 mRNA is highly expressed in the ventricular zone of E14 rat embryos (63). As classically described for VPAC1 receptors (64), the transduction pathway implicated in VA effects involves the cAMP/PKA pathway, as demonstrated by the use of H89 and forskolin. When activated, the cAMP-dependent protein kinase A releases its catalytic subunits which translocate to the nucleus and induce cellular gene expression by phosphorylating CREB (65). CREB then mediates the activation of cAMP-responsive genes by binding as a dimer to a conserved cAMP-responsive element (CRE), TGACGTCA (66-68). Of interest, the search for such TGACGTCA palindromic octamers in 50kb of genomic DNA upstream of all seven mouse *Mcph* genes revealed the presence of three distinct CRE sequences in *Mcph1* (located at 15.2kb, 19.6kb and 37kb upstream of the first exon), one CRE sequence in *Wdr62* (located at 15kb upstream of the first exon), and one CRE sequence in *Cep152* (4.88 kb upstream of the first exon), but failed to reveal any CRE sequence upstream of *Cdk5rap2*, *Aspm*, *Cenpj* and *Stil*. These findings

support the idea that the specific *Mcph1* regulation by VIP involves the cAMP/PKA pathway. We can not exclude that other transduction pathways are involved in VIP effects since i) VIP has been shown to activate other pathways including PKC and MAPK pathways (69), and ii) our preliminary screen of transduction inhibitors showed that PKC blockade, but not MAPK blockade, partially reversed VIP effects (data not shown).

How does *Mcph1* down-regulation lead to blockade of neural cell proliferation?

MCPH1 has been shown to regulate the expression of *CHK1* and *BRCA1* (14, 15). In the present study, inhibition of *Mcph1*, through VA or direct gene silencing, induced a down-regulation of *Chk1* and *Brca1* in neural progenitors both in vivo and in vitro. Since the effects of VA and *Mcph1* inhibition on *Chk1* expression were of a larger amplitude than those observed on *Brca1* expression, we focused our study on *Chk1* inhibition and its impact on progenitor proliferation although future studies will be necessary to determine whether *Brca1* inhibition participates as well to the reduced proliferation observed with VA treatment.

CHK1, when activated through the phosphorylation of several C-terminal residues, displays a kinase activity, inducing phosphorylation of numerous downstream proteins including key cell cycle regulators (58, 59). In addition, more recent data support the hypothesis that CHK1 binds to chromatin and has a direct transcriptional activity (70-72). In terms of biological effects, a large body of literature implicates CHK1 in DNA repair (58, 73). However, more recently, CHK1 has also been shown to regulate the cell cycle of cells with undamaged DNA, through a mechanism most likely independent (phosphorylation at a different residue) from DNA repair (22, 25, 60, 61, 74). Indeed, depletion of CHK1 in somatic cells under unperturbed conditions induces S phase arrest and repression of *cyclin B1* and *cdk1* expression (70). Interestingly, $Chk1^{-/-}$ mice die at E6.5, further supporting a role of CHK1 during normal embryonic development (75). In the present study, we provide

experimental data supporting the hypothesis that down-regulation of *Chk1* is sufficient to slow down the proliferation of neural progenitors. The underlying mechanism could involve phosphorylation of proteins controlling the mitotic cycle through Chk1 kinase activity and/or transcription of genes controlling cell cycle progression such as, the cyclin-dependent cyclin *Cdc25* and *cyclin B,* and the cyclin-dependent kinase *Cdk1*. Of interest, in agreement with previous studies showing that CHK1 depletion induces S phase (70), the present study shows that VA treatment induces a S phase lengthening of VZ neural progenitors.

What are the clinical implications of the modulation of neural cell proliferation by a maternal factor?

In neural progenitors, the cell cycle is regulated in a tight, specific and timely manner (for review, (76)) and the molecular mechanisms underlying this control seem to be largely conserved through evolution of mammals (77-79).

VIP has previously been shown to be a maternal factor acting on early brain development in rodents (80). Similarly, some data also suggest that maternal VIP could act on the embryonic and foetal brain in humans (41). Here, we demonstrate that administration of VA to pregnant mice during neurogenesis induces embryonic microcephaly with as much as 20% reduction of overall cortical thickness. This VA effect is mediated through the regulation of the expression and/or function of *Mcph1* and *Chk1*, which are important regulators of cell cycle. Our data strongly suggest that environmental factors, including maternal ones, can influence the tightly controlled molecular machinery of neural progenitor proliferation. Comparable modulation of this intrinsic molecular machinery has been described for irradiation that induces murine microcephaly through *Aspm* gene inhibition (81). Altogether, these data raise the hypothesis that other environmental factors could impinge on the intrinsic control of neural progenitor proliferation and therefore modulate the final size of the brain.

MATERIAL AND METHODS

Animals

All animal experiments were carried out according to protocols approved by the institutional review committee (Bichat-Robert Debré ethical committee, Paris, France) and meet INSERM guidelines as well as the Guide for the Care and use of Laboratory Animals as promulgated and adopted by the NIH, USA. All the main experiments were performed in Swiss mice (Elevage Janvier).

The day of vaginal plug was considered E0.5. Pregnant mice were killed by cervical dislocation. Embryos were harvested in cold PBS and fixed over night in freshly prepared 4% paraformaldehyde / 0,12M Phosphate Buffer (PFA 4%). For immunohistochemistry, they were then either dehydrated in ascending grades of ethanol and embedded in paraffin or cryoprotected in 10% sucrose/0,12M Phosphate Buffer overnight and embedded in 7.5% Gelatine/10% Sucrose solution, prior to flash freezing in isopentane. Tissues were later cut sagitally at 10µm on cryostat or coronally at 7µm on microtome. Newborn and adult animals were anesthetised with isofurane and intracardiacally perfused with a NaCl 9‰ solution followed by PFA4%. Brains were dissected and post fixed either overnight in PFA 4% and cryopreserved in Gelatine/Sucrose, or in 4% Formol for 4 days prior to embedding in paraffin. For in situ hybridization, embryos were fixed in PFA 4% overnight, then cryoprotected in 30% sucrose/0,12M Phosphate Buffer overnight and embedded in 7.5% Gelatine/30% Sucrose solution, frozen in isopentane and cut coronally at 10µm. In situ hybridization was performed according to Ravassard et al. (82) using a digoxigenin-labeled RNA antisense probe corresponding to nt 1-1146 of *Mcph1*.

Animal injections

Pregnant swiss mice were injected intraperitoneally twice a day (8-9 AM and 6-7 PM) between E9.5 and E11.5 with 50µl of either PBS (vehicle), or VIP Antagonist (VA, hybrid of VIP and Neurotensin which is a competitive antagonist of VIP receptors (83), or again VIP, according to the original protocol designed by Gressens et al. (1993). Both peptides were purchased from Bachem and injected at the final concentration of 2µg/g body weight.

Cell cycle study, BrdU and iododeoxyuridin (IdU) injections

On embryonic Day E11.5, IdU was injected one hour after the latest VA injection into pregnant females followed by BrdU injections (50mg/g body weight ea.) performed 90min later. Dams were sacrificed 2 hours after the IdU injection according to the original protocol schematically depicted on Figure 2C. Embryos were fixed with PFA4%, cut (10µm cryostat sections) and processed for double immunostaining (see below). Sections were immunolabeled with monoclonal anti BrdU antibodies raised in mouse or rat that recognized either the two analogues or BrdU alone, respectively.

Histology, Immunohistochemistry

Histopathological feature of embryonic telencephalon or brains were studied by analyzing E11.5, E12.5 and P5 control or treated Swiss mice. Tissues were processed for histology and immunohistochemistry as described in Supplemental Methods. BrdU and p27kip1 antibodies were from Becton Dickinson Ltd, USA, BrdU and DCX antibodies from Abcam Ltd, Calretinin and Calbindin antibodies from Swant Ltd, NeuN antibody from Chemicon Ltd, GFAP antibody from Dako Ltd, cleaved Caspase3 antibody from Cell Signaling Ltd, Cux1 antibody from Santa Cruz Ltd, Satb2 and Tbr1 antibodies from Abcam, Ltd. TUNEL was performed using the In Situ Cell Death Detection kit, Fluorescein from Roche Ltd.

Quantifications

Quantification of cortical thickness, surface and NeuN stainings was performed on primary somatosensory cortex (S1)(see Supplemental Methods). Quantification of DAPI, BrdU-IdU C-Caspase3 and p27kip1 (at E11,5), DCX and Calretinin (at E12.5) staining was performed on images from the dorsal telencephalon (see Supplemental Methods). For all quantifications, the embryos and brains (6 to 8 per group) were taken from at least 2 litters.

Neurosphere-derived progenitors culture

Primary neural stem cell cultures or neurospheres were established from forebrain of embryos at gestation E10.5 using trypsin dissociation as described in Supplemental Methods.

Drug administration was performed at DIV 3 after the first passage of neurospheres. Neural stem cells were harvested at 4 and 20 hours after treatment for BrdU experiments and RNA extraction, respectively. Peptides including VIP, VA, VPAC1 agonist ($VIP_{[A11A22A28]}$) (64), VPAC2 agonist ($VIP_{[A19K27K28]}$) (84) were used at final concentrations ranging from 10pM to 1µM, while signaling modulators such as H-89 and forskolin (FSK, Calbiochem Ltd) were used at 20 and 30µM respectively.

Cell proliferation studies

BrdU incorporation assay (cell proliferation kit, Roche Ltd) was performed on neurospheres derived progenitors according to manufacturer's instructions as described in Supplemental Methods.

Western Blot

Freshly-excised cortices were soaked into 2x cell lysis buffer purchased from Cell Signaling and supplemented with protease inhibitors including 1mM sodium orthovanadate (Na3VO4),

1µg/ml leupeptin and 10µM PMSF. Total proteins, 20 or 60 ug /lane, for cell and tissue extracts, respectively were loaded onto 12% SDS-polyacrylamide gels and transferred to nitrocellulose membranes (GE Healthcare Ltd). Membranes were probed with mouse anti-actin (1/10,000, Chemicon Ltd), rabbit anti MCPH1 (1/500, Abcam Ltd), rabbit anti CDK5RAP2 (1/2000, Bethyl Ltd), rabbit anti ASPM (1/200, Novus Ltd), rabbit ant CENPJ (1/800, Abcam Ltd), rabbit anti STIL (1/500, Abcam Ltd), goat anti-CHK1 and mouse BRCA1 (1/200, Chemicon) antibodies (1/1,000, R&D Ltd). Antibodies were revealed by horseradish peroxydase-coupled conjugates and the staining intensity was analyzed with ImageJ program (NIH).

RNA extraction and relative quantification of gene expression by Real time PCR

Samples were isolated from animals aging from E12 to P40. Forebrains and cortices were carefully dissected and total RNA was extracted according to a previously published protocol (85). After reverse-transcription performed using iScript cDNA kit from Biorad Ltd, real-time RT-PCR were performed using protocols and reagents described elsewhere (86). Primer sequences used for quantitative RT-PCR are listed in Table 2 from Supplemental Methods.

Kinase assay

Chk1 kinase assay was performed on telencephalon or cortices extracts or neurosphere-derived progenitors using Active Chk1 kinase IP-kinase assay (DuoSet IC, R&D Systems) according to the manufacturer instructions as described in Supplemental Methods.

Lentiviral transduction

A set of three lentiviral vectors carrying different shRNAs targeting *Mcph1* and four lentiviral vectors carrying different shRNAs targeting *Chk1* were purchased from Sigma Aldrich Ltd.

They are provided as ready-to-use lentiviral particles. The shRNA corresponding sequences are given in Table 3 (Supplemental Methods). Neurosphere-derived progenitors were transduced by lentiviral particles according to manufacturer recommendations as described in Supplemental Methods.

Statistical analysis

Quantitative data are expressed as mean ± SEM for each treatment group. Results were compared using Student's *t*-tests or ANOVA with Bonferroni's multiple comparison of means test (GraphPad Prism, GraphPad Software). A $p<0.05$ was considered as significant.

Acknowledgements

This work was supported by Inserm, CNRS, Université Paris Diderot, Université de Strasbourg, APHP (Contrat d'Interface to Dr P. Gressens), Fondation Lejeune, Fondation Grace de Monaco, Fondation pour la Recherche Médicale, Société Française de Neuropédiatrie, Journées de Neurologie de Langue Française, and IFCPAR-CEFIPRA (project number 3803-3 to Drs S. Mani and P. Gressens). We thank Gaëlle Friocourt for instructions on BrdU-IdU immunohistochemistry.

REFERENCES

1. Aicardi, J. 1998. Malformations of the central nervous system in childhood. In *Diseases of the nervous system in childhood*. London: Mac Keith press. p90-91.
2. Kaindl, A.M., Passemard, S., Kumar, P., Kraemer, N., Issa, L., Zwirner, A., Gerard, B., Verloes, A., Mani, S., and Gressens, P. Many roads lead to primary autosomal recessive microcephaly. *Prog Neurobiol.* 2010;90(3):363-83.
3. Passemard, S., Kaindl, A.M., Titomanlio, L., Gerard, B., Gressens, P., and Verloes, A. Primary Autosomal Recessive Microcephaly. . *GeneReviews at GeneTests. Medical Genetics Information Resource [database online]. Copyright, University of Washington, Seattle, 1997-2009.*

Available at http://www.genetests.org. . 2009.
4. Jackson, A.P., Eastwood, H., Bell, S.M., Adu, J., Toomes, C., Carr, I.M., Roberts, E., Hampshire, D.J., Crow, Y.J., Mighell, A.J., et al. Identification of microcephalin, a protein implicated in determining the size of the human brain. *Am J Hum Genet.* 2002; 71(1):136-142.
5. Bilguvar, K., Ozturk, A.K., Louvi, A., Kwan, K.Y., Choi, M., Tatli, B., Yalnizoglu, D., Tuysuz, B., Caglayan, A.O., Gokben, S., et al. Whole-exome sequencing identifies recessive WDR62 mutations in severe brain malformations. *Nature.* 2010; 467(7312):207-210.
6. Nicholas, A.K., Khurshid, M., Desir, J., Carvalho, O.P., Cox, J.J., Thornton, G., Kausar, R., Ansar, M., Ahmad, W., Verloes, A., et al. WDR62 is associated with the spindle pole and is mutated in human microcephaly. *Nat Genet.* 2010; 42(11):1010-1014.
7. Yu, T.W., Mochida, G.H., Tischfield, D.J., Sgaier, S.K., Flores-Sarnat, L., Sergi, C.M., Topcu, M., McDonald, M.T., Barry, B.J., Felie, J.M., et al. Mutations in WDR62, encoding a centrosome-associated protein, cause microcephaly with simplified gyri and abnormal cortical architecture. *Nat Genet.* 2010; 42(11):1015-1020.
8. Bond, J., Roberts, E., Springell, K., Lizarraga, S.B., Scott, S., Higgins, J., Hampshire, D.J., Morrison, E.E., Leal, G.F., Silva, E.O., et al. A centrosomal mechanism involving CDK5RAP2 and CENPJ controls brain size. *Nat Genet.* 2005; 37(4):353-355.
9. Guernsey, D.L., Jiang, H., Hussin, J., Arnold, M., Bouyakdan, K., Perry, S., Babineau-Sturk, T., Beis, J., Dumas, N., Evans, S.C., et al. Mutations in centrosomal protein CEP152 in primary microcephaly families linked to MCPH4. *Am J Hum Genet.* 2010; 87(1):40-51.
10. Bond, J., Roberts, E., Mochida, G.H., Hampshire, D.J., Scott, S., Askham, J.M., Springell, K., Mahadevan, M., Crow, Y.J., Markham, A.F., et al. ASPM is a major determinant of cerebral cortical size. *Nat Genet.* 2002; 32(2):316-320.
11. Kumar, A., Girimaji, S.C., Duvvari, M.R., and Blanton, S.H. Mutations in STIL, encoding a pericentriolar and centrosomal protein, cause primary microcephaly. *Am J Hum Genet.* 2009; 84(2):286-290.
12. Alderton, G.K., Galbiati, L., Griffith, E., Surinya, K.H., Neitzel, H., Jackson, A.P., Jeggo, P.A., and O'Driscoll, M. Regulation of mitotic entry by microcephalin and its overlap with ATR signalling. *Nat Cell Biol.* 2006; 8(7):725-733.

13. Erez, A., Chaussepied, M., Castiel, A., Colaizzo-Anas, T., Aplan, P.D., Ginsberg, D., and Izraeli, S. The mitotic checkpoint gene, SIL is regulated by E2F1. *Int J Cancer.* 2008; 123(7):1721-1725.
14. Lin, S.Y., Rai, R., Li, K., Xu, Z.X., and Elledge, S.J. BRIT1/MCPH1 is a DNA damage responsive protein that regulates the Brca1-Chk1 pathway, implicating checkpoint dysfunction in microcephaly. *Proc Natl Acad Sci U S A.* 2005; 102(42):15105-15109.
15. Xu, X., Lee, J., and Stern, D.F. Microcephalin is a DNA damage response protein involved in regulation of CHK1 and BRCA1. *J Biol Chem.* 2004; 279(33):34091-34094.
16. Pfaff, K.L., Straub, C.T., Chiang, K., Bear, D.M., Zhou, Y., and Zon, L.I. The zebra fish cassiopeia mutant reveals that SIL is required for mitotic spindle organization. *Mol Cell Biol.* 2007; 27(16):5887-5897.
17. Zhong, X., Liu, L., Zhao, A., Pfeifer, G.P., and Xu, X. The abnormal spindle-like, microcephaly-associated (ASPM) gene encodes a centrosomal protein. *Cell Cycle.* 2005; 4(9):1227-1229.
18. Zhong, X., Pfeifer, G.P., and Xu, X. Microcephalin encodes a centrosomal protein. *Cell Cycle.* 2006; 5(4):457-458.
19. Gowen, L.C., Johnson, B.L., Latour, A.M., Sulik, K.K., and Koller, B.H. Brca1 deficiency results in early embryonic lethality characterized by neuroepithelial abnormalities. *Nat Genet.* 1996; 12(2):191-194.
20. Kalay, E., Yigit, G., Aslan, Y., Brown, K.E., Pohl, E., Bicknell, L.S., Kayserili, H., Li, Y., Tuysuz, B., Nurnberg, G., et al. CEP152 is a genome maintenance protein disrupted in Seckel syndrome. *Nat Genet.* 2010; 43(1):23-26.
21. Kramer, A., Mailand, N., Lukas, C., Syljuasen, R.G., Wilkinson, C.J., Nigg, E.A., Bartek, J., and Lukas, J. Centrosome-associated Chk1 prevents premature activation of cyclin-B-Cdk1 kinase. *Nat Cell Biol.* 2004; 6(9):884-891.
22. Loffler, H., Rebacz, B., Ho, A.D., Lukas, J., Bartek, J., and Kramer, A. Chk1-dependent regulation of Cdc25B functions to coordinate mitotic events. *Cell Cycle.* 2006; 5(21):2543-2547.
23. Rai, R., Dai, H., Multani, A.S., Li, K., Chin, K., Gray, J., Lahad, J.P., Liang, J., Mills, G.B., Meric-Bernstam, F., et al. BRIT1 regulates early DNA damage response, chromosomal integrity, and cancer. *Cancer Cell.* 2006; 10(2):145-157.
24. Rai, R., Phadnis, A., Haralkar, S., Badwe, R.A., Dai, H., Li, K., and Lin, S.Y. Differential regulation of centrosome integrity by DNA damage response proteins. *Cell Cycle.* 2008; 7(14):2225-2233.
25. Tang, J., Erikson, R.L., and Liu, X. Checkpoint kinase 1 (Chk1) is required for mitotic progression through negative regulation of polo-like kinase 1 (Plk1). *Proc Natl Acad Sci U S A.* 2006; 103(32):11964-11969.
26. Izraeli, S., Lowe, L.A., Bertness, V.L., Good, D.J., Dorward, D.W., Kirsch, I.R., and Kuehn, M.R. The SIL gene is required for mouse embryonic axial development and left-right specification. *Nature.* 1999; 399(6737):691-694.
27. Lam, M.H., Liu, Q., Elledge, S.J., and Rosen, J.M. Chk1 is haploinsufficient for multiple functions critical to tumor suppression. *Cancer Cell.* 2004; 6(1):45-59.
28. Liang, Y., Gao, H., Lin, S.Y., Peng, G., Huang, X., Zhang, P., Goss, J.A., Brunicardi, F.C., Multani, A.S., Chang, S., et al. BRIT1/MCPH1 is essential for mitotic and meiotic recombination DNA repair and maintaining genomic stability in mice. *PLoS Genet.* 2010; 6(1):e1000826.
29. Trimborn, M., Ghani, M., Walther, D.J., Dopatka, M., Dutrannoy, V., Busche, A., Meyer, F., Nowak, S., Nowak, J., Zabel, C., et al. Establishment of a Mouse Model

with Misregulated Chromosome Condensation due to Defective Mcph1 Function. *PLoS One.* 2010; 5(2):e9242.
30. Feng, Y., and Walsh, C.A. Mitotic spindle regulation by Nde1 controls cerebral cortical size. *Neuron.* 2004; 44(2):279-293.
31. Cuzon, V.C., Yeh, P.W., Yanagawa, Y., Obata, K., and Yeh, H.H. Ethanol consumption during early pregnancy alters the disposition of tangentially migrating GABAergic interneurons in the fetal cortex. *J Neurosci.* 2008; 28(8):1854-1864.
32. Marret, S., Gressens, P., Van-Maele-Fabry, G., Picard, J., and Evrard, P. Caffeine-induced disturbances of early neurogenesis in whole mouse embryo cultures. *Brain Res.* 1997; 773(1-2):213-216.
33. Sadraie, S.H., Kaka, G.R., Sahraei, H., Dashtnavard, H., Bahadoran, H., Mofid, M., Nasab, H.M., and Jafari, F. Effects of maternal oral administration of morphine sulfate on developing rat fetal cerebrum: a morphometrical evaluation. *Brain Res.* 2008; 1245:36-40.
34. Sargeant, T.J., Day, D.J., Miller, J.H., and Steel, R.W. Acute in utero morphine exposure slows G2/M phase transition in radial glial and basal progenitor cells in the dorsal telencephalon of the E15.5 embryonic mouse. *Eur J Neurosci.* 2008; 28(6):1060-1067.
35. Takano, T., Akahori, S., Takeuchi, Y., and Ohno, M. Neuronal apoptosis and gray matter heterotopia in microcephaly produced by cytosine arabinoside in mice. *Brain Res.* 2006; 1089(1):55-66.
36. Griffith, E., Walker, S., Martin, C.A., Vagnarelli, P., Stiff, T., Vernay, B., Al Sanna, N., Saggar, A., Hamel, B., Earnshaw, W.C., et al. Mutations in pericentrin cause Seckel syndrome with defective ATR-dependent DNA damage signaling. *Nat Genet.* 2008; 40(2):232-236.
37. Cote, F., Fligny, C., Bayard, E., Launay, J.M., Gershon, M.D., Mallet, J., and Vodjdani, G. Maternal serotonin is crucial for murine embryonic development. *Proc Natl Acad Sci U S A.* 2007; 104(1):329-334.
38. Mairet-Coello, G., Tury, A., and DiCicco-Bloom, E. Insulin-like growth factor-1 promotes G(1)/S cell cycle progression through bidirectional regulation of cyclins and cyclin-dependent kinase inhibitors via the phosphatidylinositol 3-kinase/Akt pathway in developing rat cerebral cortex. *J Neurosci.* 2009; 29(3):775-788.
39. Sahara, S., and O'Leary, D.D. Fgf10 regulates transition period of cortical stem cell differentiation to radial glia controlling generation of neurons and basal progenitors. *Neuron.* 2009; 63(1):48-62.
40. Vitalis, T., Cases, O., Passemard, S., Callebert, J., and Parnavelas, J.G. Embryonic depletion of serotonin affects cortical development. *Eur J Neurosci.* 2007; 26(2):331-344.
41. Ottesen, B., Ulrichsen, H., Fahrenkrug, J., Larsen, J.J., Wagner, G., Schierup, L., and Sondergaard, F. Vasoactive intestinal polypeptide and the female genital tract: relationship to reproductive phase and delivery. *Am J Obstet Gynecol.* 1982; 143(4):414-420.
42. Spong, C.Y., Lee, S.J., McCune, S.K., Gibney, G., Abebe, D.T., Alvero, R., Brenneman, D.E., and Hill, J.M. Maternal regulation of embryonic growth: the role of vasoactive intestinal peptide. *Endocrinology.* 1999; 140(2):917-924.
43. Gressens, P., Hill, J.M., Gozes, I., Fridkin, M., and Brenneman, D.E. Growth factor function of vasoactive intestinal peptide in whole cultured mouse embryos. *Nature.* 1993; 362(6416):155-158.

44. Gressens, P., Hill, J.M., Paindaveine, B., Gozes, I., Fridkin, M., and Brenneman, D.E. Severe microcephaly induced by blockade of vasoactive intestinal peptide function in the primitive neuroepithelium of the mouse. *J Clin Invest.* 1994; 94(5):2020-2027.
45. Gozes, I., McCune, S.K., Jacobson, L., Warren, D., Moody, T.W., Fridkin, M., and Brenneman, D.E. An antagonist to vasoactive intestinal peptide affects cellular functions in the central nervous system. *J Pharmacol Exp Ther.* 1991; 257(3):959-966.
46. Gozes, I., Meltzer, E., Rubinrout, S., Brenneman, D.E., and Fridkin, M. Vasoactive intestinal peptide potentiates sexual behavior: inhibition by novel antagonist. *Endocrinology.* 1989; 125(6):2945-2949.
47. Moody, T.W., Zia, F., Draoui, M., Brenneman, D.E., Fridkin, M., Davidson, A., and Gozes, I. A vasoactive intestinal peptide antagonist inhibits non-small cell lung cancer growth. *Proc Natl Acad Sci U S A.* 1993; 90(10):4345-4349.
48. Gressens, P., Paindaveine, B., Hill, J.M., Evrard, P., and Brenneman, D.E. Vasoactive intestinal peptide shortens both G1 and S phases of neural cell cycle in whole postimplantation cultured mouse embryos. *Eur J Neurosci.* 1998; 10(5):1734-1742.
49. Martynoga, B., Morrison, H., Price, D.J., and Mason, J.O. Foxg1 is required for specification of ventral telencephalon and region-specific regulation of dorsal telencephalic precursor proliferation and apoptosis. *Dev Biol.* 2005; 283(1):113-127.
50. Quinn, J.C., Molinek, M., Martynoga, B.S., Zaki, P.A., Faedo, A., Bulfone, A., Hevner, R.F., West, J.D., and Price, D.J. Pax6 controls cerebral cortical cell number by regulating exit from the cell cycle and specifies cortical cell identity by a cell autonomous mechanism. *Dev Biol.* 2007; 302(1):50-65.
51. Takahashi, T., Nowakowski, R.S., and Caviness, V.S., Jr. The cell cycle of the pseudostratified ventricular epithelium of the embryonic murine cerebral wall. *J Neurosci.* 1995; 15(9):6046-6057.
52. Nguyen, L., Besson, A., Heng, J.I., Schuurmans, C., Teboul, L., Parras, C., Philpott, A., Roberts, J.M., and Guillemot, F. p27kip1 independently promotes neuronal differentiation and migration in the cerebral cortex. *Genes Dev.* 2006; 20(11):1511-1524.
53. Francis, F., Koulakoff, A., Boucher, D., Chafey, P., Schaar, B., Vinet, M.C., Friocourt, G., McDonnell, N., Reiner, O., Kahn, A., et al. Doublecortin is a developmentally regulated, microtubule-associated protein expressed in migrating and differentiating neurons. *Neuron.* 1999; 23(2):247-256.
54. Brenneman, D.E., Westbrook, G.L., Fitzgerald, S.P., Ennist, D.L., Elkins, K.L., Ruff, M.R., and Pert, C.B. Neuronal cell killing by the envelope protein of HIV and its prevention by vasoactive intestinal peptide. *Nature.* 1988; 335(6191):639-642.
55. Vaudry, D., Gonzalez, B.J., Basille, M., Yon, L., Fournier, A., and Vaudry, H. Pituitary adenylate cyclase-activating polypeptide and its receptors: from structure to functions. *Pharmacol Rev.* 2000; 52(2):269-324.
56. Huen, M.S., Sy, S.M., and Chen, J. BRCA1 and its toolbox for the maintenance of genome integrity. *Nat Rev Mol Cell Biol.* 2010; 11(2):138-148.
57. Mullan, P.B., Quinn, J.E., and Harkin, D.P. The role of BRCA1 in transcriptional regulation and cell cycle control. *Oncogene.* 2006; 25(43):5854-5863.
58. Reinhardt, H.C., and Yaffe, M.B. Kinases that control the cell cycle in response to DNA damage: Chk1, Chk2, and MK2. *Curr Opin Cell Biol.* 2009; 21(2):245-255.
59. Sancar, A., Lindsey-Boltz, L.A., Unsal-Kacmaz, K., and Linn, S. Molecular mechanisms of mammalian DNA repair and the DNA damage checkpoints. *Annu Rev Biochem.* 2004; 73:39-85.
60. Wilsker, D., and Bunz, F. Chk1 phosphorylation during mitosis: a new role for a master regulator. *Cell Cycle.* 2009; 8(8):1161-1163.

61. Wilsker, D., Petermann, E., Helleday, T., and Bunz, F. Essential function of Chk1 can be uncoupled from DNA damage checkpoint and replication control. *Proc Natl Acad Sci U S A.* 2008; 105(52):20752-20757.
62. Zachos, G., Black, E.J., Walker, M., Scott, M.T., Vagnarelli, P., Earnshaw, W.C., and Gillespie, D.A. Chk1 is required for spindle checkpoint function. *Dev Cell.* 2007; 12(2):247-260.
63. Basille, M., Vaudry, D., Coulouarn, Y., Jegou, S., Lihrmann, I., Fournier, A., Vaudry, H., and Gonzalez, B. Comparative distribution of pituitary adenylate cyclase-activating polypeptide (PACAP) binding sites and PACAP receptor mRNAs in the rat brain during development. *J Comp Neurol.* 2000; 425(4):495-509.
64. Laburthe, M., Couvineau, A., and Tan, V. Class II G protein-coupled receptors for VIP and PACAP: structure, models of activation and pharmacology. *Peptides.* 2007; 28(9):1631-1639.
65. Mayr, B., and Montminy, M. Transcriptional regulation by the phosphorylation-dependent factor CREB. *Nat Rev Mol Cell Biol.* 2001; 2(8):599-609.
66. Comb, M., Birnberg, N.C., Seasholtz, A., Herbert, E., and Goodman, H.M. A cyclic AMP- and phorbol ester-inducible DNA element. *Nature.* 1986; 323(6086):353-356.
67. Montminy, M.R., Sevarino, K.A., Wagner, J.A., Mandel, G., and Goodman, R.H. Identification of a cyclic-AMP-responsive element within the rat somatostatin gene. *Proc Natl Acad Sci U S A.* 1986; 83(18):6682-6686.
68. Short, J.M., Wynshaw-Boris, A., Short, H.P., and Hanson, R.W. Characterization of the phosphoenolpyruvate carboxykinase (GTP) promoter-regulatory region. II. Identification of cAMP and glucocorticoid regulatory domains. *J Biol Chem.* 1986; 261(21):9721-9726.
69. Laburthe, M., Couvineau, A., and Marie, J.C. VPAC receptors for VIP and PACAP. *Receptors Channels.* 2002; 8(3-4):137-153.
70. Shimada, M., Niida, H., Zineldeen, D.H., Tagami, H., Tanaka, M., Saito, H., and Nakanishi, M. Chk1 is a histone H3 threonine 11 kinase that regulates DNA damage-induced transcriptional repression. *Cell.* 2008; 132(2):221-232.
71. Smits, V.A. Spreading the signal: dissociation of Chk1 from chromatin. *Cell Cycle.* 2006; 5(10):1039-1043.
72. Smits, V.A., Reaper, P.M., and Jackson, S.P. Rapid PIKK-dependent release of Chk1 from chromatin promotes the DNA-damage checkpoint response. *Curr Biol.* 2006; 16(2):150-159.
73. Stracker, T.H., Usui, T., and Petrini, J.H. Taking the time to make important decisions: the checkpoint effector kinases Chk1 and Chk2 and the DNA damage response. *DNA Repair (Amst).* 2009; 8(9):1047-1054.
74. Petermann, E., and Caldecott, K.W. Evidence that the ATR/Chk1 pathway maintains normal replication fork progression during unperturbed S phase. *Cell Cycle.* 2006; 5(19):2203-2209.
75. Liu, Q., Guntuku, S., Cui, X.S., Matsuoka, S., Cortez, D., Tamai, K., Luo, G., Carattini-Rivera, S., DeMayo, F., Bradley, A., et al. Chk1 is an essential kinase that is regulated by Atr and required for the G(2)/M DNA damage checkpoint. *Genes Dev.* 2000; 14(12):1448-1459.
76. Dehay, C., and Kennedy, H. Cell-cycle control and cortical development. *Nat Rev Neurosci.* 2007; 8(6):438-450.
77. Evans, P.D., Mekel-Bobrov, N., Vallender, E.J., Hudson, R.R., and Lahn, B.T. Evidence that the adaptive allele of the brain size gene microcephalin introgressed into Homo sapiens from an archaic Homo lineage. *Proc Natl Acad Sci U S A.* 2006; 103(48):18178-18183.

78. Gilbert, S.L., Dobyns, W.B., and Lahn, B.T. Genetic links between brain development and brain evolution. *Nat Rev Genet.* 2005; 6(7):581-590.
79. Hill, R.S., and Walsh, C.A. Molecular insights into human brain evolution. *Nature.* 2005; 437(7055):64-67.
80. Hill, J.M., McCune, S.K., Alvero, R.J., Glazner, G.W., Henins, K.A., Stanziale, S.F., Keimowitz, J.R., and Brenneman, D.E. Maternal vasoactive intestinal peptide and the regulation of embryonic growth in the rodent. *J Clin Invest.* 1996; 97(1):202-208.
81. Fujimori, A., Yaoi, T., Ogi, H., Wang, B., Suetomi, K., Sekine, E., Yu, D., Kato, T., Takahashi, S., Okayasu, R., et al. Ionizing radiation downregulates ASPM, a gene responsible for microcephaly in humans. *Biochem Biophys Res Commun.* 2008; 369(3):953-957.
82. Ravassard, P., Chatail, F., Mallet, J., and Icard-Liepkalns, C. Relax, a novel rat bHLH transcriptional regulator transiently expressed in the ventricular proliferating zone of the developing central nervous system. *J Neurosci Res.* 1997; 48(2):146-158.
83. Gozes, Y., Brenneman, D.E., Fridkin, M., Asofsky, R., and Gozes, I. A VIP antagonist distinguishes VIP receptors on spinal cord cells and lymphocytes. *Brain Res.* 1991; 540(1-2):319-321.
84. Langer, I., Gregoire, F., Nachtergael, I., De Neef, P., Vertongen, P., and Robberecht, P. Hexanoylation of a VPAC2 receptor-preferring ligand markedly increased its selectivity and potency. *Peptides.* 2004; 25(2):275-278.
85. Fontaine, R.H., Cases, O., Lelievre, V., Mesples, B., Renauld, J.C., Loron, G., Degos, V., Dournaud, P., Baud, O., and Gressens, P. IL-9/IL-9 receptor signaling selectively protects cortical neurons against developmental apoptosis. *Cell Death Differ.* 2008; 15(10):1542-1552.
86. Favrais, G., Couvineau, A., Laburthe, M., Gressens, P., and Lelievre, V. Involvement of VIP and PACAP in neonatal brain lesions generated by a combined excitotoxic/inflammatory challenge. *Peptides.* 2007; 28(9):1727-1737.

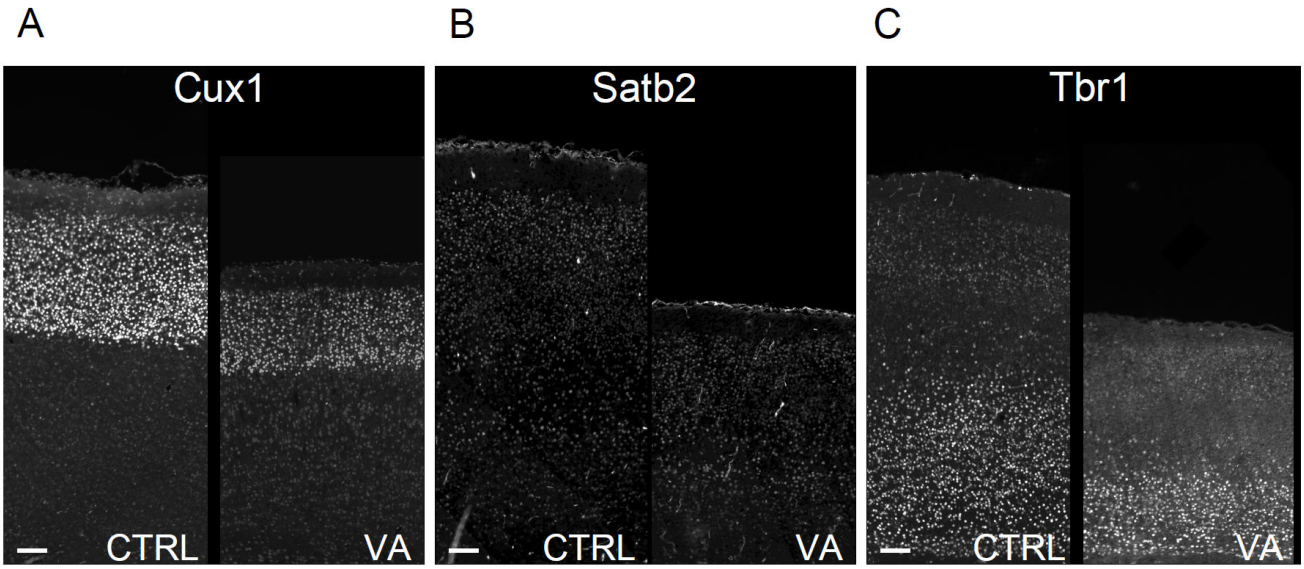

Figure 1: VIP blockade during neurogenesis induces microcephaly with thinner cortex and reduction of both upper and lower cortical layers.
A-C: Coronal P6 brain sections immunostained with specific markers of cortical layers (A: Cux1; B: Satb2; C: Tbr1) shows that all layers are reduced in thickness in VA-treated animals when compared to age matched controls (Scale bar = 100μm).

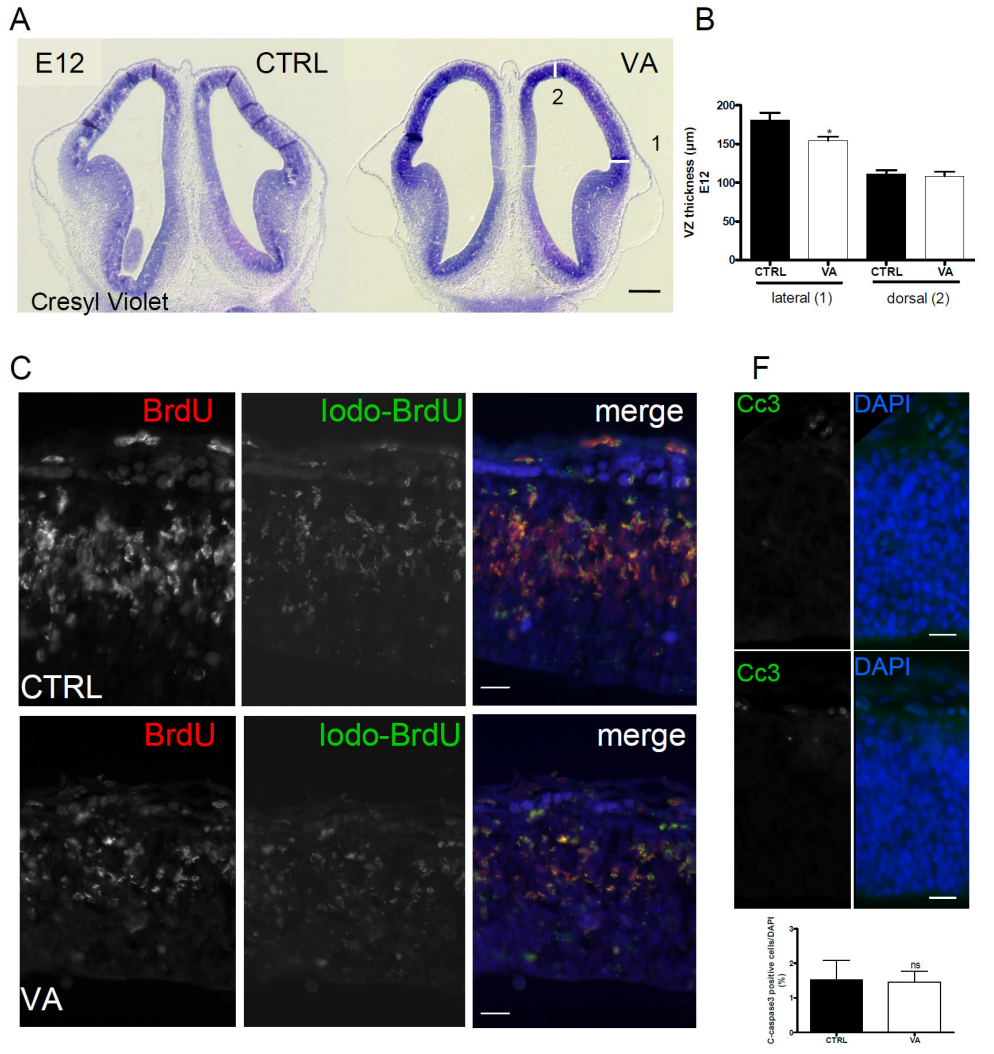

E

Dorsal E11,5	Ts (h)	Tc (h)	Ts/Tc
CTRL	5,4±0,38	12±0,76	0,45±0,02
VA	8,5±0,87	29±4	0,30±0,02
p value	0,0317	0,0159	0,0159

Figure 2: VA reduces cortical thickness in embryos by lengthening cell cycle during neurogenesis without inducing excess apoptosis.

A: Coronal section of Control and VA brains from E12.5 embryos stained by Cresyl Violet (scale bar 200 µm).

B: Lateral and dorsal cortical thickness of E12.5 embryo telencephalon in Control and VA groups (n=6, unpaired t-test, p< 0.05*).

C: Double labelling BrdU (red), IdU (green) and Dapi (blue) at E11.5 in the dorsal telencephalic Ventricular Zone (VZ) in Control and VA sections (scale bar 20 µm).

D: schematic representation of experimental BrdU-IdU procedure: Injection at T0 h with IdU and at T1.5 h (Ti) with BrdU followed by sacrifice at T2.0 h allows identification of the three cell types shown on C : those within the S-phase at T0–1.5 but within G2/M at T1.5–2.0 (labeled in green due to IdU-incorporation only = Leaving fraction = *Lcells* = IdU+/BrdU-); cells entering S-phase at T1.5–2.0 (labeled in red because of BrdU incorporation = BrdU+/IdU-); and finally cells within S-phase at both T0 and T1.5 (labeled in yellow due to IdU/BrdU incorporation = S fraction = *Scells* = IdU+/BrdU+). DAPI counterstained nuclei in blue (*Pcells*).

E: Cell cycle parameters (Mean±SEM) calculated from IdU/BrdU double labeling according to (45) : Lenght of S phase = Ts = Ti/(*Lcells*/*Scells*); Total cell time = Tc = Ts/(*Scells*/*Pcells*). In VZ progenitors cells, both S phase and total cell cycle of VA treated embryos are lengthened (8.5h vs 5.4 and 29h vs 12h respectively; n=5, unpaired t-test).

F: Immunostaining for cleaved-caspase-3 does not show any difference between CTRL and VA treated animals (n=8 par group, t-test, p<0.05*). Scale bar 20µm.

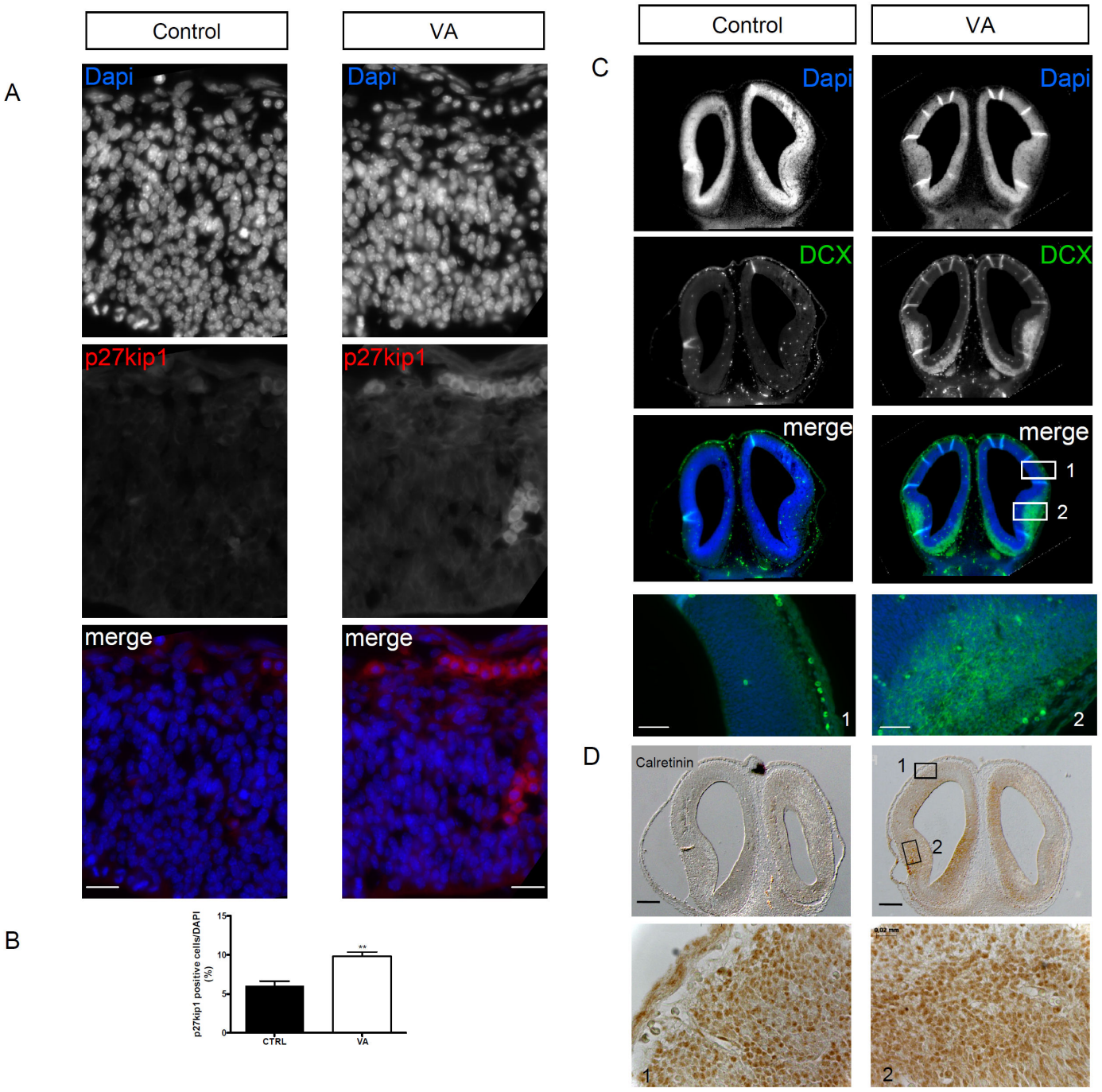

Figure 3: VA-induced microcephaly triggers cell cycle exit and early differentiation of cortical progenitors in embryos.

A-B: Immunofluorescent staining for p27kip1 on coronal E11.5 sections in dorsal telencephalon of VA-treated embryos compared to controls (Figure 3A, Scale bar: 20µm). The labeling index (number of p27kip1-positive cells over the total number of nuclei stained by DAPI) is increased in VA-treated embryos as compared to controls (n=7 per group, unpaired t-test, $p< 0.01$**).

C: Immunofluorescent staining for DCX on coronal E12.5 sections in dorsal telencephalon of VA-treated embryos compared to controls. Post-mitotic DCX positive neurons are observed in VA-treated embryos in lateral ganglionic eminence (LGE) and in the dorsal, medial and lateral preplate while positive staining remained almost absent in controls at E12.5. (scale bar: 200 µm). Lower panel shows high magnification pictures of DCX-immunoreactive cells in box 1 and 2 (scale bar: 50µm).

D: Calretinin immunoreactivity at the same level as mentioned above. Note the intense labeling in LGE (box 2) and in the dorsal (box 1), medial and lateral preplate, which are undetectable in controls. (scale bar: 200 µm). Lower panel shows high magnification pictures of calretinin-immunoreactive cells in box 1 and 2.

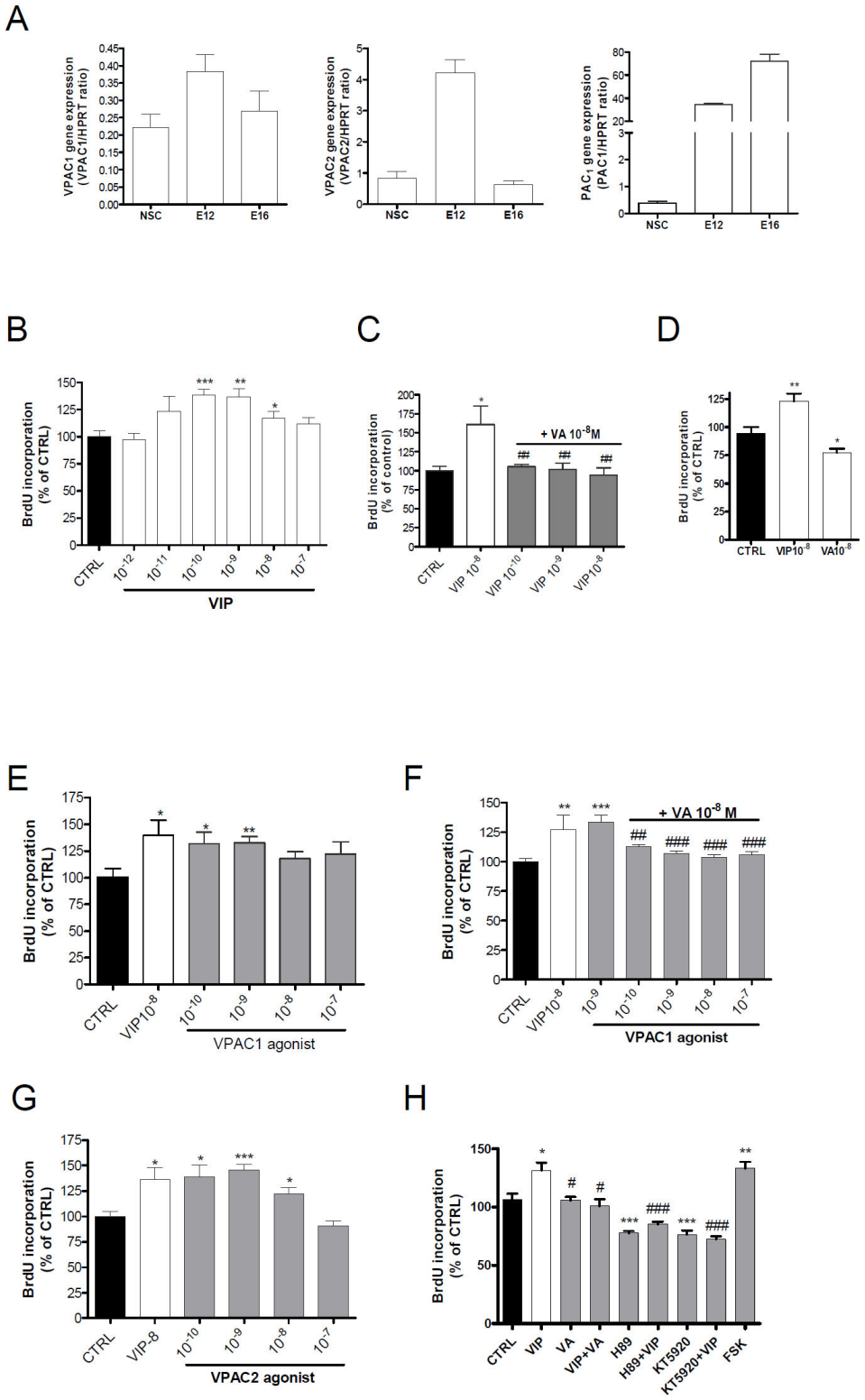

Figure 4: VA acts by interfering with VIP/VPAC signalling pathway and PKA activation.
A: VIP receptors, VPAC1 and VPAC2 expression levels as assessed by quantitative RT-PCR performed from neurosphere-derived progenitors and E12/E16 telecephalon. VPAC1 and VPAC2 receptors are mainly expressed in early stages while PAC1 expression increased throughout the development.
B-H: BrdU incorporation assay performed on E10.5 neurosphere-derived progenitors. VIP stimulates proliferation of E10.5 neurosphere-derived progenitors in a dose-dependent manner (Figure 4B). This effect is completely abrogated by VA at concentration as low as 0.1nM (Figure 4C). VA alone decreases proliferation of neurosphere-derived progenitors compared to PBS (D). VPAC1 (Figures 4E-F) and VPAC2 (Figure 4G) agonists mimic VIP-induced BrdU incorporation. VIP stimulatory effect on BrdU incorporation is mimicked by the adenylate-cyclase activator forskolin (FSK) but is inhibited by H89 or KT5920, two separate inhibitors of PKA (Figure 4H). (n=8 per group, unpaired t-test, $p< 0.05$*, 0.01** or 0.001*** between treatments and controls, or $p< 0.05^{\#}$, $0.01^{\#\#}$ or $0.001^{\#\#\#}$ between VIP and other treatments)

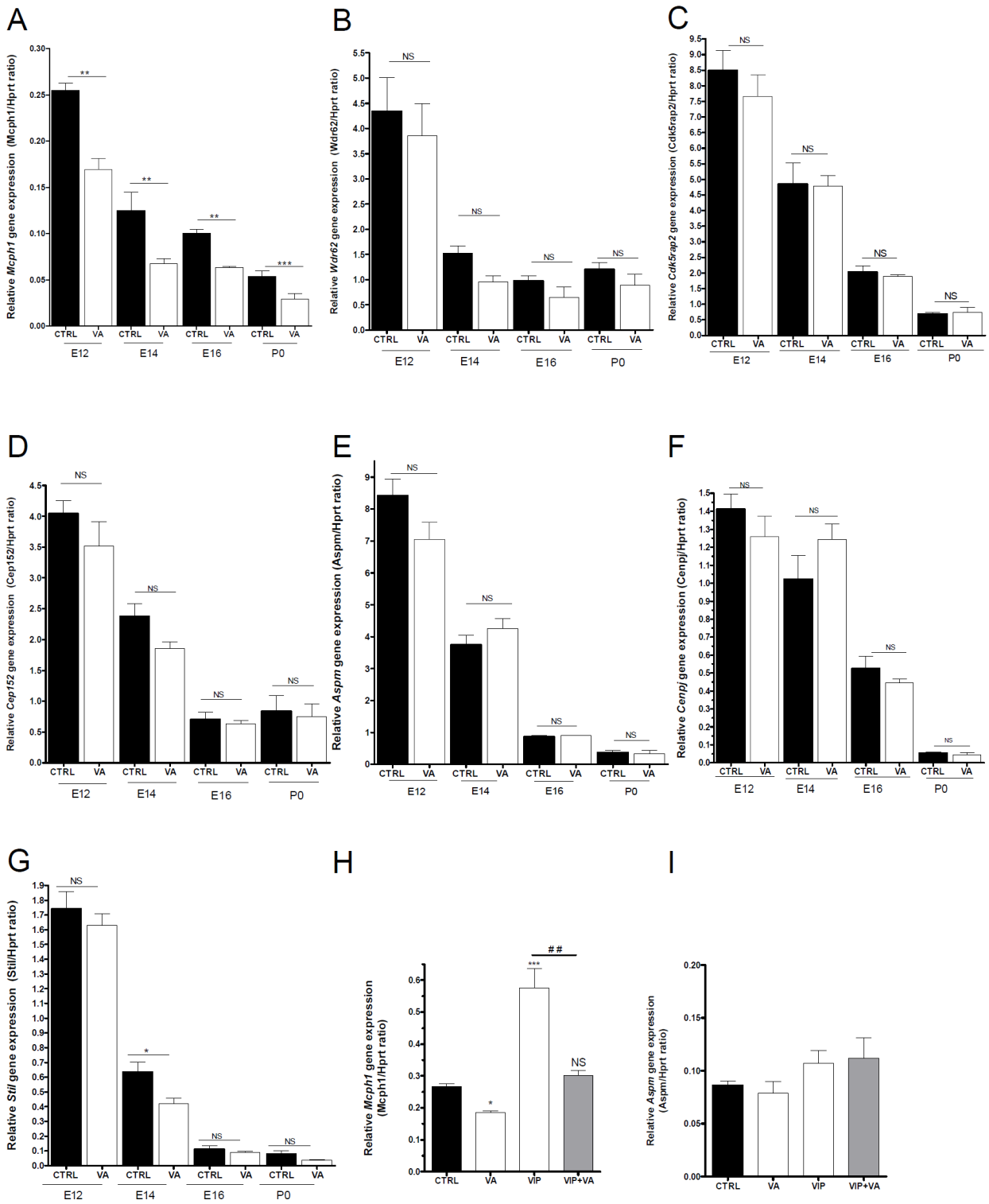

Figure 5: VA treatment affects specifically the expression of *Mcph1* gene *in vivo*.

A-E: Expression levels of all known *Mcph* genes: *Mcph1* (A), *Wdr62* (B), *Cdk5rap2* (C), *Cep152* (D), *Aspm* (E), *Cenpj* (F) and *Stil* (G) assessed by quantitative RT-PCR on RNA samples extracted from telencephalon of embryos (CTRL or VA-treated) from E12 to P0. Parallel to the time-dependent reduction in *Mcph* gene expression, VA induced a significant decrease in *Mcph1* expression (n=8, run in duplicate, one-way ANOVA followed by Bonferroni post-test, $p<0.05$*, 0.01** or 0.001***) compared to controls (A). In contrast no clear difference was observed between CTRL and VA samples at the corresponding ages for *Wdr62, Cdk5rap2, Cep152, Aspm*, *Cenpj* and *Stil* **(B-G)**.

H-I: Rescue experiments performed on E16 telencephalic samples by quantitative RT-PCR. *Mcph1* transcription (H) is also up-regulated by VIP ($p<0.05$*, 0.01** or 0.001***), while co-injection of VA significantly represses VIP-induced over-expression ($p< 0.05^{\#}$, $0.01^{\#\#}$ or $0.001^{\#\#\#}$). *Aspm* expression used herein as negative control remains unaffected by VIP, VA or both (I).

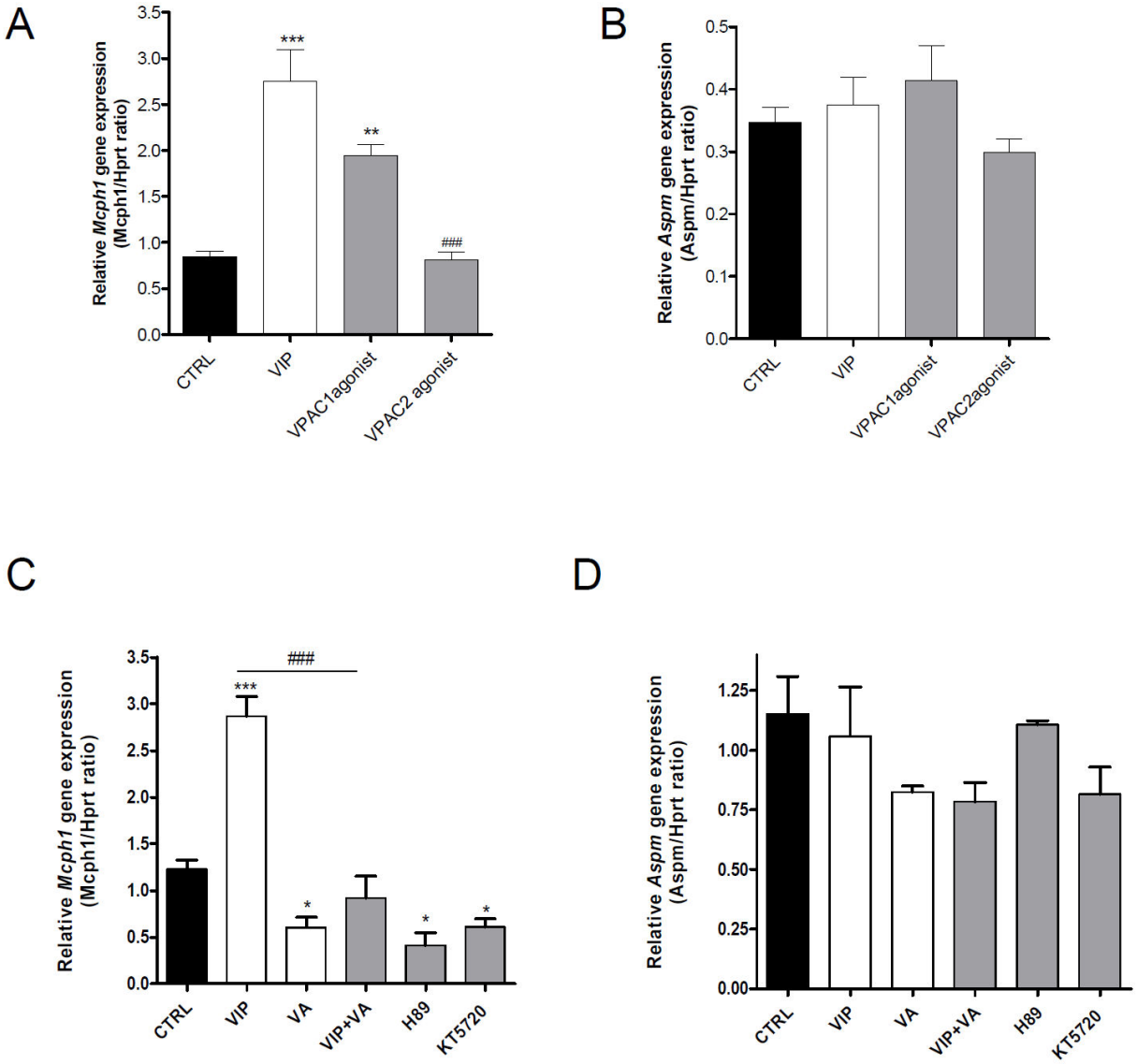

Figure 6: VA treatment affects *Mcph1* gene expression in E10.5 neurosphere-derived progenitors through VPAC1-PKA signaling.

A-B: *Mcph1* and *Aspm* (used as control) expression levels assessed by quantitative RT-PCR isolated from neurosphere cultures treated with VIP analogues. Note that only VPAC1 agonist was able to perfectly mimic VIP effects (n=4 per group, run in duplicate, one-way ANOVA, $p<0.05$*, 0.01** or 0.001***). Once again, VPAC1 agonist failed to induce any change *Aspm* expression.

C-D: Similar to the above experiment, neurosphere cultures were treated with VIP, VA, VIP+VA, VIP+H89, KT5720, two PKA inhibitors, to analyse *Mcph1* or *Aspm* gene expression. VIP-induced stimulation of transcript levels (Mean±SEM) compared to controls (n=4 per group, run in duplicate, one-way ANOVA, $p<0.05$*, 0.01** or 0.001***), VA reduces *Mcph1* transcript expression. VIP effects on *Mcph1* expression is abolished in the presence of VA ($p< 0.05^{\#}$, $0.01^{\#\#}$ or $0.001^{\#\#\#}$). Three inhibitors of PKA reduce *Mcph1* expression, mimicking VA effects. *Aspm* gene expression was not modified by these treatments.

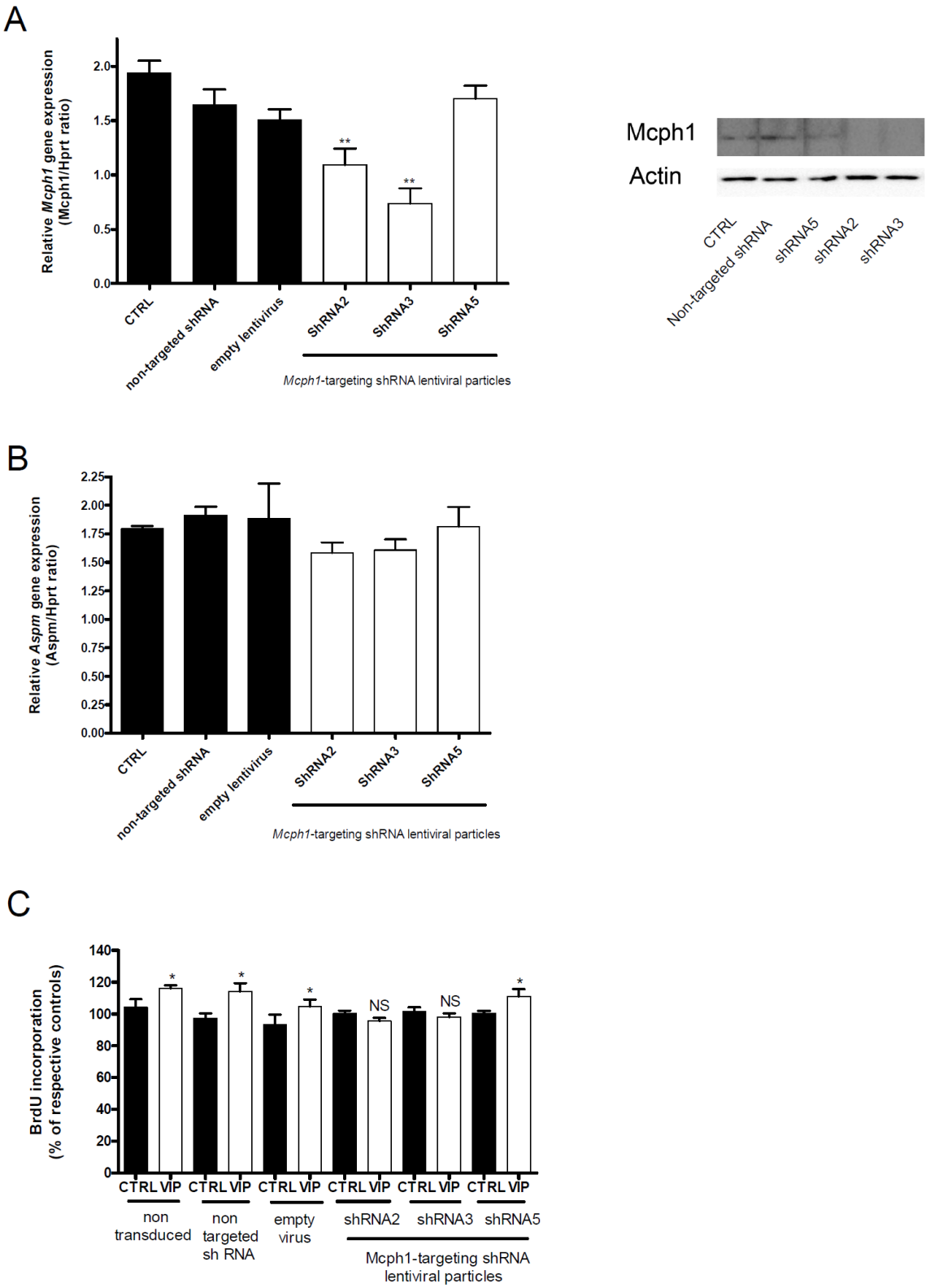

Figure 7: *Mcph1* silencing reproduced VA effects on VIP-induced proliferation of neural progenitors.
A-B: *Mcph1* and *Aspm* gene expression as assessed by quantitative RT-PCR from neurosphere-derived progenitors transduced by *Mcph1* specific lentiviral-mediated shRNA *Mcph1*-specific shRNA2 and 3 inhibit specifically *Mcph1* transcript expression (n=3 per group, one-way ANOVA, $p<0.05$*, 0.01** or 0.001***). The negative controls (empty virus and non target shRNA) failed to modulate *Mcph1* expression. Knock down of *Mcph1* by shRNA2 and 3 results in lost of Mcph1 protein at DIV5 post- transduction (A, right panel). Knock down of *Mcph1* fails to affect *Aspm* expression (B).
C: BrdU incorporation by neurosphere-derived progenitors treated by *Mcph1* specific shRNA in the presence of VIP or PBS (control). Note that *Mcph1* shRNA2 and 3 abolishes VIP-induced proliferation.

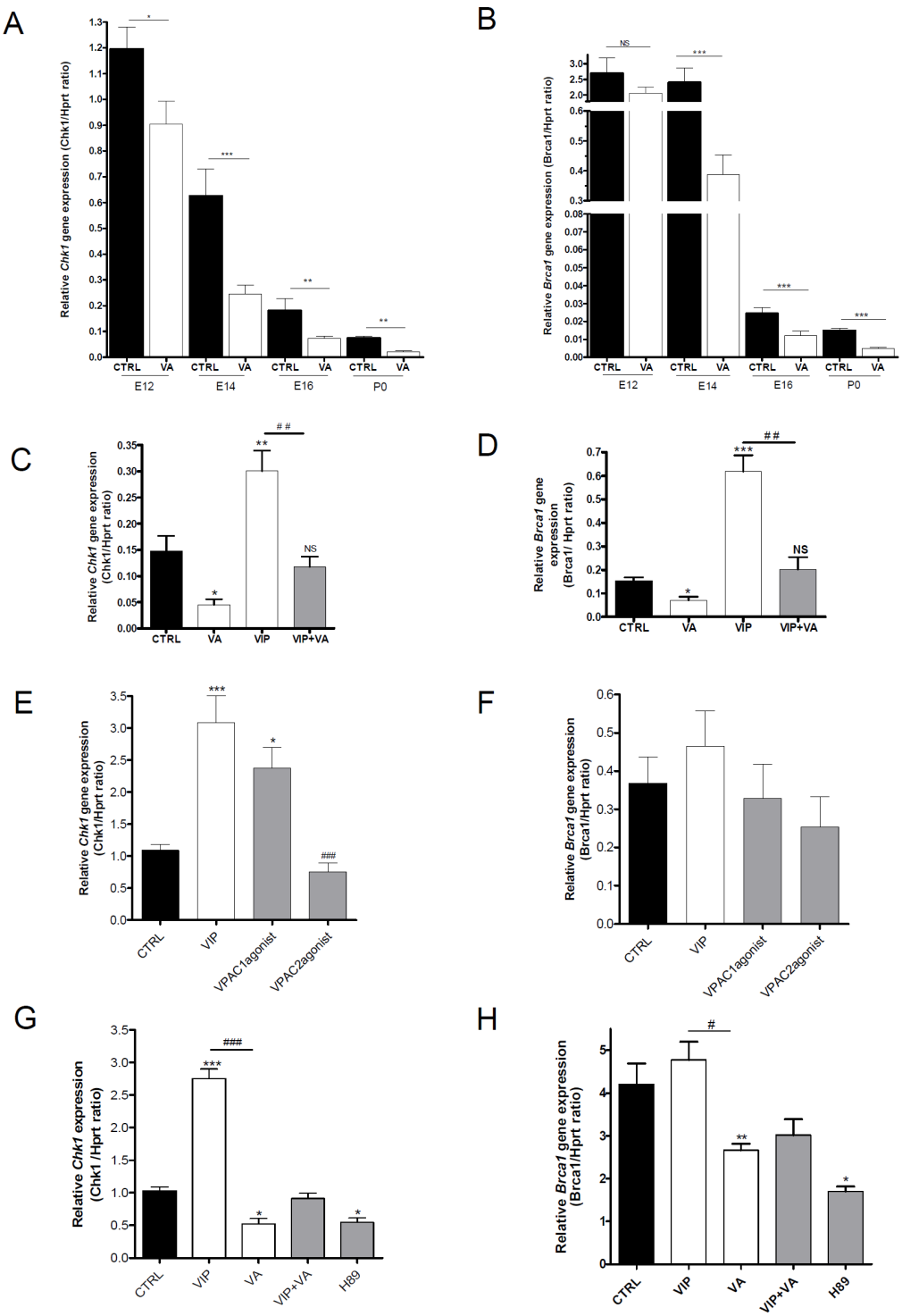

Figure 8: **VA treatment reduces *Chk1* and *Brca1* gene expression both *in vivo* and *in vitro*.**
A-D: *Chk1* and *Brca1* expression levels assessed by quantitative RT-PCR on RNA samples extracted from telencephalon of embryos (CTRL or VA-treated) from E12 to P0. VA induced a significant decrease in *Chk1* (A) and *Brca1* (B) expression (n=8 per group, one-way ANOVA followed by Bonferroni post-test, $p<0.05$*, 0.01** or 0.001***). In rescue experiments performed at E16 by quantitative RT-PCR, VIP up-regulates both *Chk1* and *Brca1*, while co-injection of VA and VIP significantly represses VIP-induced over-expression of both genes (at $p< 0.05^{\#}$, $0.01^{\#\#}$ or $0.001^{\#\#\#}$) (C and D).
E-H: *Chk1* and *Brca1* expression levels in neurosphere-derived progenitors. *Chk1* is upregulated by VIP and blocked by VA (E, G). VPAC1 agonist increases *Chk1* transcript level, whereas VPAC2 agonist has no effect (E). VIP increases mildly *Brca1* gene expression (F, H), while VA reduces significantly *Brca1* gene expression. H89 inhibits both *Chk1* and *Brca1* gene expression (G, H), mimicking VA effects.

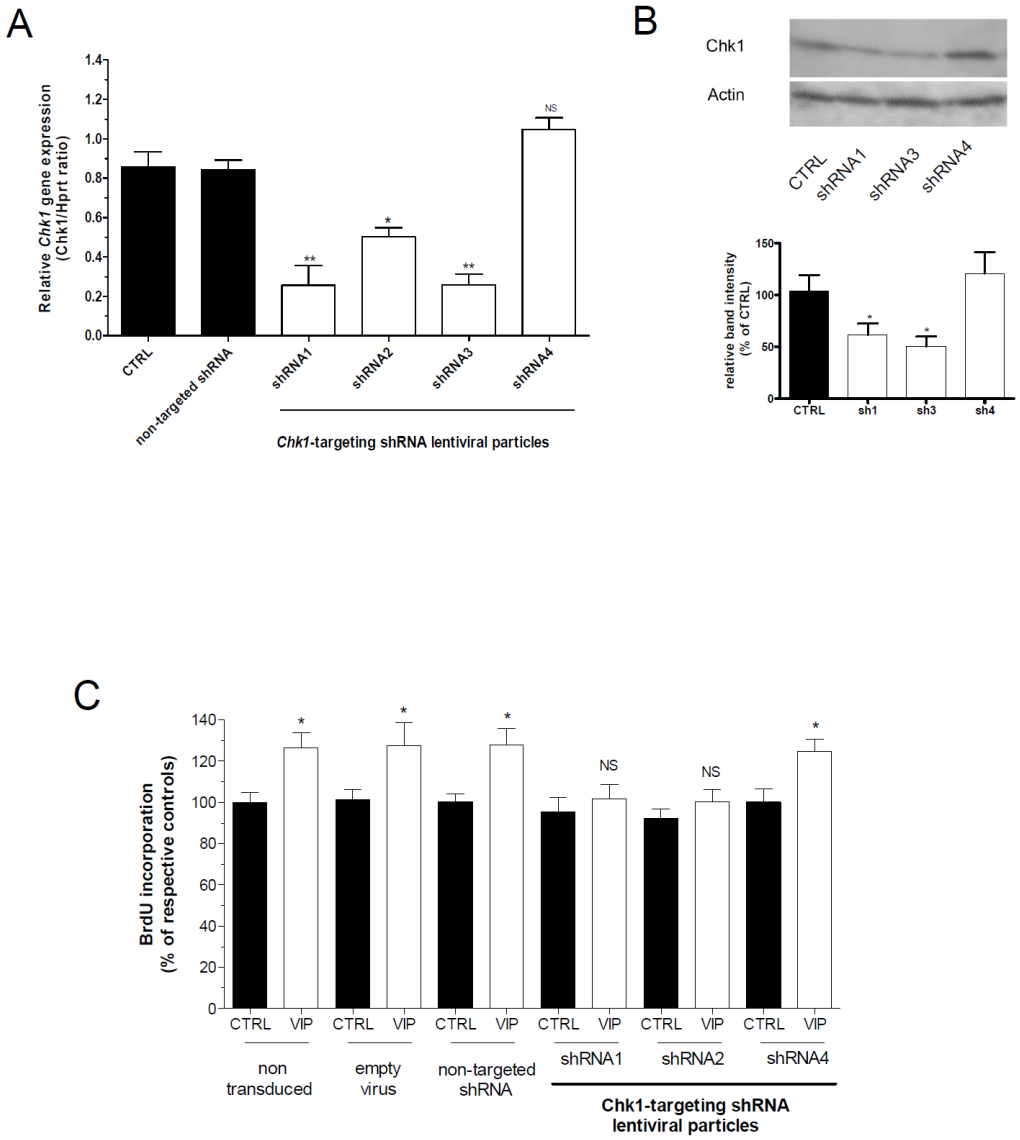

Figure 9: The effects of VIP on neurosphere proliferation are abolished in the absence of *Chk1*.
A-B: *Chk1* expression levels assessed by quantitative RT-PCR on extracts from neurosphere-derived progenitors transduced by lentiviral-mediated specific *Chk1* specific shRNA. Knock-down of *Chk1* gene expression by sequences shRNA1, 2 and 3 significantly reduces both mRNA levels (**A**) and protein contents (**B**), while sequence shRNA4 failed to induce any significant silencing.
C: BrdU incorporation in neurosphere-derived progenitors transduced by different control lentiviral vectors and the specific *Chk1*-shRNA1 and 2. Silencing *chk1* gene obliterates VIP-induced mitogenic action in neurosphere-derived progenitors.

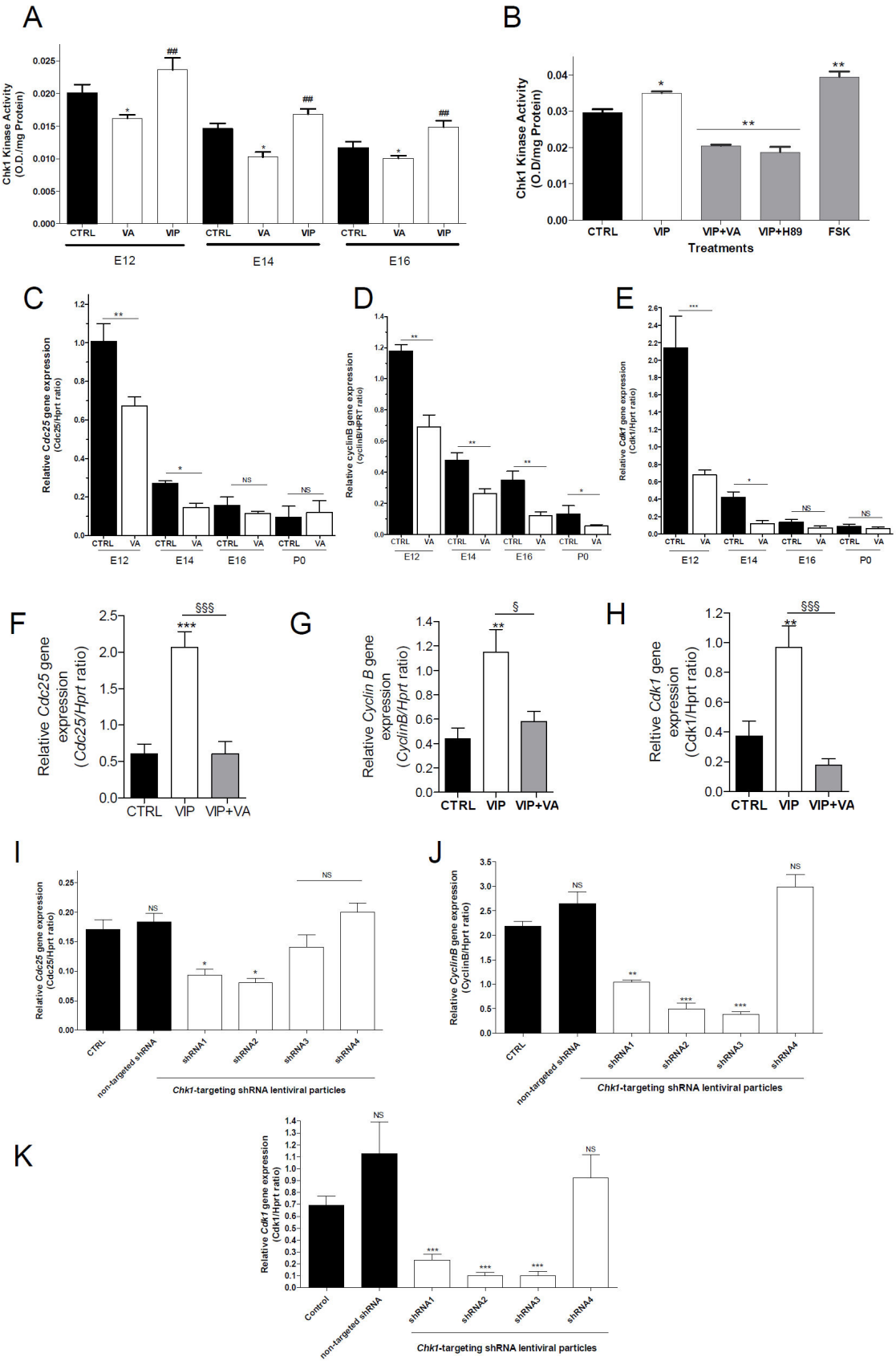
A
Chk1 Kinase Activity (O.D./mg Protein)
CTRL
VA
VIP
E12
E14
E16
B
Chk1 Kinase Activity (O.D/mg Protein)
CTRL
VIP
VIP+VA
VIP+H89
FSK
Treatments
C
Relative Cdc25 gene expression (Cdc25/Hprt ratio)
D
Relative cyclinB gene expression (cyclinB/HPRT ratio)
E
Relative Cdk1 gene expression (Cdk1/Hprt ratio)
E12
E14
E16
P0
F
Relative Cdc25 gene expression (Cdc25/Hprt ratio)
G
Relative Cyclin B gene expression (CyclinB/Hprt ratio)
H
Reltive Cdk1 gene expression (Cdk1/Hprt ratio)
I
Relative Cdc25 gene expression (Cdc25/Hprt ratio)
J
Relative CyclinB gene expression (CyclinB/Hprt ratio)
non-targeted shRNA
shRNA1
shRNA2
shRNA3
shRNA4
Chk1-targeting shRNA lentiviral particles
K
Relative Cdk1 gene expression (Cdk1/Hprt ratio)
Control

Figure 10: Chk1 kinase activity and expression of key cell cycle regulators downstream of *Chk1* are reduced by VA.

A: Chk1 kinase activity assessed by kinase essay on telencephalon or cortical extracts from E12 to P0 embryos and newborns, that received VA, VIP or both treatments. At the three embryonic ages, Chk1 kinase activity (Mean ±SEM) follows the same time-dependent decrease in controls. VIP treatment stimulates Chk1 activity (n=5 per group, run in duplicate, one-way ANOVA, $p< 0.05^{\#}$, $0.01^{\#\#}$ or $0.001^{\#\#\#}$), while VA suppresses it ($p<0.05$*, 0.01** or 0.001***).

B: Chk1 kinase activity on protein extracts isolated from neurosphere cultures after treatment with VIP or VIP+VA or again cAMP/PKA agents. VIP stimulates kinase activity in neurospheres ($p<0.05$*); such an enhancement was counterbalanced by co-treatment VIP+VA ($p<0.01$**). H89 inhibited the kinase activity ($p<0.01$**), while FSK enhanced it ($p<0.01$**).

C-E: Transcription levels of specific key cell cycle regulators downstream of *Chk1* (*Cdc25, cyclin A/B Cdk1 and Cdk2* genes) assessed by quantitative RT-PCR. Only *Cdc25, CyclinB* and *Cdk1* transcripts are significantly repressed (n=8, one-way ANOVA, $p<0.05$* or $p< 0.01$**) by VA treatment, but no change in *Cdk2*, and *Cyclin A* levels (not shown).

F-H: Similar experiments conducted in neurosphere-derived progenitors. VIP upregulates *Cdc25* (F) *Cyclin B* (G) and *Cdk1* (H) expression and this effect was inhibited by VA treatment.

I-K: Efficient *Chk1*-targetting by lentiviral mediated vectors expressing shRNAs (1, -2, and -3) down-regulated *Cdc25* (I) *cyclin B* (J) and *Cdk1* (K) expression (n=3, run in duplicate, one-way ANOVA, $p<0.05$*, 0.01** or 0.001***).

SUPPLEMENTAL INFORMATION

SUPPLEMENTAL METHODS

Histology, immunohistochemistry

Embryos and brains were dissected and fixed following the above-mentioned protocol. Paraffin sections were dewaxed, rehydrated and stained with 0.1% cresyl violet.

For deoxyuridine derivatives and p27Kip1, brains were fixed with PFA4%, cryoprotected with 10-30% of sucrose and cryo-sectioned at 10µm. For BrdU-IdU experiments, sections were treated with 2N HCl for 30 min at 37°C, wash in PBS three times. For all immunohistochemical staining, sections were blocked with 10% serum for one hour and incubated more than 2 hours at room temperature with specific monoclonal antibody including mouse anti-BrdU (and IdU) (1/50), p27Kip1(1/1000) primary antibodies from Becton Dickinson Ltd, rabbit anti cleaved-caspase3 (1/200) from Cell Signaling Ltd, goat anti-Cux1 (1/100, Santa Cruz Ltd), mouse anti-Satb2 (1/100), rabbit anti-Tbr1 (1/500), or rat monoclonal anti-BrdU (1/200) from Abcam Ltd. Secondary antibodies used were either Cy3-conjugated goat anti-rat IgM (1/500) or goat anti-mouse conjugates labelled with Alexa-488 (1/1000) or -546 (1/500) purchased from Invitrogen Ltd.

For paraffin-embedded embryos or brains, coronal sections were dipped in ascending grades of ethanol. Slides were microwaved in 10mM sodium citrate, blocked for an hour in 10% serum before an overnight incubation with the following primary antibodies: mouse anti-NeuN (NeuN) (1/500, Chemicon Ltd), rabbit anti-Calretinin (1/2000, Swant Ltd), rabbit anti-Glial Fibrillary Acidic Protein (GFAP) (1/1000, Dako Ltd), rabbit anti-Caspase 3 (1/200, Cell Signaling Ltd), rabbit anti-Doublecortin (DCX) (1/200, Abcam Ltd). All antibodies were polyclonal except for NeuN.

After a first incubation with biotinylated anti rabbit or anti mouse IgG 1% (1/100) followed by a second incubation with avidin-biotin-peroxydase complex (ABC kit, Vectastain, Vector laboratories, Ltd) the final detection of the peroxydase reaction was obtained with diaminobenzidine as chromogen (Sigma, Ltd) according to manufacturer's recommendations.

All images were collected with confocal microscopy or optic microscopy (Zeiss, Ltd) and processed using Axiovision (Zeiss) or Photoshop (Adobe) softwares.

Quantifications

Cortical thickness at P5 was measured on coronal sections at rostral (1) and caudal (2) levels of the primary somatosensory cortex (The mouse brain in stereotaxic coordinates, G. Paxinos and KBJ Franklin, 2004, compact second edition, Elsevier, level: Interaural/Bregma 4.90/1.10 and 1.98/-1.82 respectively). The thickness of primary somatosensory cortical layers II-IV and layers V-VI were measured from coronal sections at the same level as mentioned above (level 2). Cortical surface was measured at the same age, from the cingulate cortex to the rhinal sulcus (at mouse Paxinos Atlas level Interaural/Bregma 3.94/-0.94, n=5 per condition), using Image J (NIH).

Quantification of NeuN positive neurons was performed in the S1 somatosensory cortex area of P5 animals at the same levels than those mentioned above (1, 2). Three or four non serial adjacent sections were assessed at x200 magnification within a 1mm² grid, on at least 4 animals in each group.

Quantification of BrdU-IdU, p27kip1, cleaved-capase3 and DAPI was performed within the Ventricular Zone of the dorsal telencephalon on E11.5. The total number of cells stained was counted at x40 magnification into bins (perpendicular to the apical surface of the ventricular zone: 150µm in height, 90µm in lateral for BrdU and 160µm - 45µm for cleaved-caspase3 and p27kip1 experiments), in three serial non adjacent sections, on at least 6 embryos in each group.

Neurosphere-derived progenitors culture

Forebrains were dissected from E10.5 embryos in CO_2 independent medium (Gibco Ltd, US) supplemented with Penicillin (500 Units/ml of medium) Streptomycin (500µg/ml of medium) and L-Glutamine (2mM) was added. Forebrains were incubated in trypsin and DNAse-I solution for 10 min at 37°C. Digestion was stopped by addition of foetal bovin serum (FBS), and the neural tubes were transferred in a petri dish filled with CO_2 independent medium supplemented with FBS 10% and DNAse-I to carefully separate neuroepithelia from surrounding tissues. Neuroepithelia were washed with PBS, collected by centrifugation, then mechanically dissociated by pipetting and resuspended in the culture

medium [Neurobasal medium containing L-Glutamine 2mM, Penicillin (500 Units/ml of medium), Streptomycin (500µg/ml of medium), N2 supplement (Gibco Ltd) and supplemented every two days with Fibroblast Growth Factor-Basic heparin (FGF2) (12 ng/ml Sigma Ltd)]. Cells were incubated at 37°C in a humidified incubator in an atmosphere of 5% CO_2 in an unprecoated petri dish.

In these culture conditions, neural stem cells proliferate as neurospheres. Neurospheres were kept floating until day in vitro 4 (DIV4) then harvested, dissociated first mechanically then enzymatically (TrypLE express, Invitrogen) for 20 min at 37°C and transferred in 6-, 12- or 96-well plates for quantitative PCR, western blot or BrdU experiments.

Cell proliferation studies

BrdU incorporation assay (cell proliferation kit, Roche Ltd) was performed according to manufacturer's instructions. Following the first passage of neurospheres, cells were seeded in a 96-well plate at a density of 10,000 cells per well (DIV0). On the next day (DIV1), BrdU (10µM) was added and incubation carried out for 4 hours. Then, medium was quickly removed by aspiration and cells were incubated for 30 min with FixDenat for 30 min at room temperature prior to incubation with the anti BrdU-POD working solution for 90 min. Ultimately, after washing, cells were incubated with substrate solution for 20 min. Absorbance was measured at 390 nm on Victor spectrophotometer.

Kinase assay

Chk1 kinase assay was performed using Active Chk1 kinase IP-kinase assay (DuoSet IC, R&D Systems) according to the manufacturer's instructions. Tissue samples (telencephalon or cortices from E12 to P0) or neurosphere cultures were collected and soaked in lysis buffer prior to immunoprecipitation with active Chk1 kinase antibody coated on agarose beads. Active Chk1 contained in IP pellets was finally incubated with the supplied biotinylated kinase substrate in the presence of ATP and Mg^{2+} cations for 45 min at room temperature. The kinase reaction was then stopped and detection of phosphorylated substrate was performed on streptavidin-coated 96-well plates. Colorimetric reaction was finally quantified on a microplate reader set at 450 nm.

Lentiviral-mediated cell transduction

ShRNA expressing lentiviral particles (Mission) were purchased from Sigma Aldrich Ltd. Sequences corresponding to the shRNAs are given in supplemental Table 3. Cell transduction with lentiviral particles was performed according to manufacturer's recommendations. In brief, on day 0 (DIV 0), cells were seeded in a 96-well plate at a density of 10,000 cells/well for 20 hours at 37°C. On DIV 1, medium was changed and lentiviral particles were added to the medium at multiplicity of infection (MOI) 5 for the neurosphere-derived progenitors for 20 hours. To determine the optimal virus-to-cell ratio, the MOI used corresponded to the lowest viral concentrations that still delivered the optimal transduction efficiency as established with the Turbo GFP Control lentiviral particles (Sigma Aldrich, Ltd). On DIV 3, medium was replaced with fresh medium and cells incubate for two more days. Finally, at DIV 5, cells were collected for RNA extraction or BrdU experiments and on DIV12 for protein extraction. Of note, neither puromycine selection nor hexadimethrine bromide enhancer were used in our experimental setup.

SUPPLEMENTAL TABLES

Supplemental Table 1: Calculation of the cell cycle kinetics by the IdU/BrdU double labeling

	P cells (DAPI)		L cells		S cells	
	CTRL	VA	CTRL	VA	CTRL	VA
mean	113,8	96,60	14,25	5,400	51,50	29,00
st. Error	7,793	3,444	0,4787	0,7483	3,663	1,897

CTRL (n = 4) VA (n = 5)

L cells = IdU+/BrdU-

S cells = IdU+/BrdU+

P cells = total number of proliferating cells, estimated by DAPI count in the VZ in the sampling area.

Ti = 1,5h

Ti/Ts = L cells / S cells → Ts = Ti / (L cells / S cells)

Ts/Tc = S cells / P cells → Tc = Ts / (S cells / P cells)

Supplemental Table 2: primer sequences used to specifically amplify genes of interest by quantitative RT-PCR

Genes	Primer sequences (sense and reverse)*
Mcph1	5'-GCACAGGCCTTGTCAGACCTC-OH3' 5'-GCTTCTCAGATGGCATGCTTG-OH3'
Chk1	5'-AAGCACATTCATTCCAATTTG-OH3' 5'-TGGCTGGGAACTAGAGAACTT-OH3'
Brca1	5'-CTTGTGCCCTGGGAAGACCTG-OH3' 5'-GCGCTCTTCAAATTTTGGCTT-OH3'
Wdr62	5'-ACAGGAAGCCTCCAACACC –OH3' 5'-GCATGTGAGCTCGTTGTGGAC-OH3'
Cdk5rap2	5'-TACCACCATCTCCTGCCTGA-OH3' 5'-CTGTCTGGCTTCGGGTCTCTA-OH3'
Cep152	5'- TCCGCGGGCAGTACATTA-OH3' 5'- CGCAACACTTCCGCTTTTACC-OH3'
Aspm	5'-TCCACTTTACAGCAGCTGCCT-OH3' 5'-CCATGTGCTTCTTAGCGTTCC-OH3'
Cenpj	5'-CCCAATGGAACTCGGAAAGA-OH3' 5'-CATGACCTGCTTCACATCACC-OH3'
Vpac1	5'-TCACTATGTCATGTTTGCCTT-OH3' 5'-GAAAGACCCTACGACGAGTT-OH3'
Vpac2	5'-TCTACAGCAGACCAGGAAACA-OH3' 5'-GTAGCCACACGCATCTATGAA-OH3'
Pac1	5'-ACTGCGTGGTGTCCAACTACT-OH3' 5'-TCTCCTCTCAGGGAAGAAGGT-OH3'
Cdc25	5'-CCCTCGAATGTGCCGTTCTC-OH3' 5'-CCCCCTTTGAGGATATATAGC-OH3'
Cyclin A	5'-GCTGCTAGCTTCGAAGTTTGA-OH3' 5'-AGGTGCTCCATTCTCAGAACC-OH3'
Cyclin B	5'-CAAAATACCTACAGGGTCGTG-OH3' 5'-GTCTCCTGAAGCAGCCTAAAT-OH3'
Cdk2	5'-TCCTTCACCGAGACCTTAAGC-OH3' 5'-AGTTCGGACAGGGACTCCAA-OH3'
Hprt	5'-GGTGAAAAGGACCTCTCGAA-OH3' 5'-CAAGGGCATATCCAACAACA-OH3'

*(all primer sets were designed to generate 85-110bp amplicons)

Supplemental Table 3: Lentiviral particles (controls and specific inserts) designed to assess transduction efficacy and silencing efficiency of *Chk1* expression in neurosphere-derived progenitors.

Knockdown gene	**Sh sequence/Vector description**
Empty Vector	No shRNA Insert
non target shRNA control	CCGG**CAACAAGATGAAGAGCACCAA**CTC GAG**TTGGTGCTCTTCATCTTGTTG**TTTTT
Turbo GFP Control	No shRNA insert. Contains TurboGFP gene, under the control of the CMV promoter.
Mcph1-sh1	CCG**GGCACTTGTTGATGAGTCTTTG**CTC GAG**CAAAGACTCATCAACAAGTGC**TTTTTG
Mcph1-sh2	CCG**GTGCCGACTTGAACGCCA**TTTACTC GAG**TAAATGGCGTTCAAGTCGGCA**TTTTTG
Mcph1-sh3	CCG**GCTCCTACGATGTCCATCATAG**CTC GAG**CTATGATGGACATCGTAGGAG**TTTTTG
Mcph1-sh4	CCG**GAGATACTTGTTCCCAATTATA**CTC GAG**TATAATTGGGAACAAGTATC**TTTTTTG
Mcph1-sh5	CCG**GCCACTCATCTTTCGGTGATTC**CTC GAG**GAATCACCGAAAGATGAGTGG**TTTTTG
Chk1-sh1	CCGG**GTGGAAGAAGAGTTGTATGAA**CTC GAG**TTCATACAACTCTTCTTCCAC**TTTTT
Chk1-sh2	CCGG**GCTGTGAATAGAATAACTGAA**CTC GAG**TTCAGTTATTCTATTCACAGC**TTTTT
Chk1-sh3	CCGG**GCAACGGTATTTCGGCATAAT**CTC GAG**ATTATGCCGAAATACCGTTGC**TTTTT
Chk1-sh4	CCGG**GCCACGAGAATGTAGTGAAAT**CTC GAG**ATTTCACTACATTCTCGTGGC**TTTTT
Chk1-sh5	CCGG**CCCATGTAGTAGTATCACTTT**CTC GAG**AAAGTGATACTACTACATGGG**TTTTT

SUPPLEMENTAL FIGURES

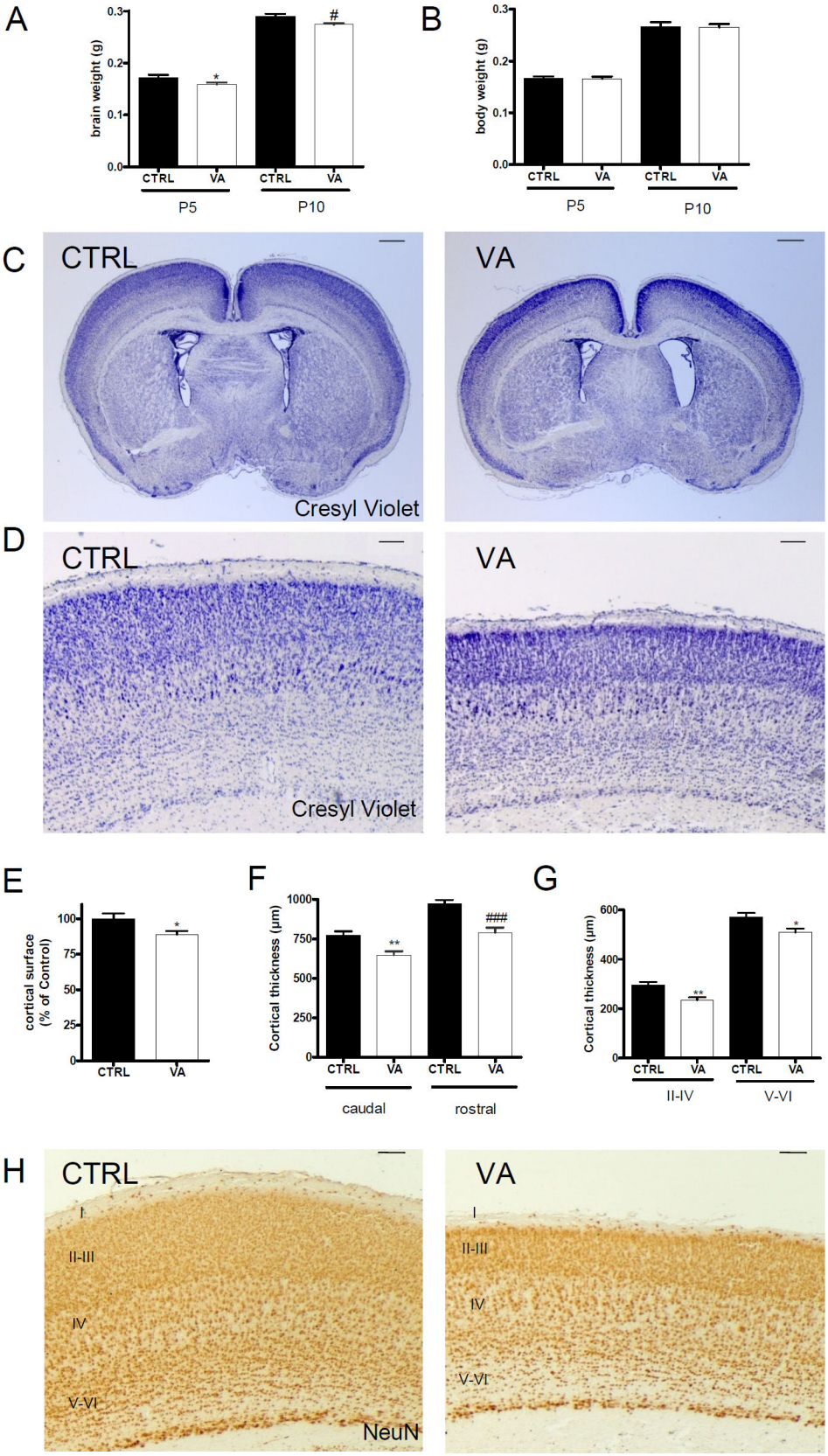

Supplemental Figure 1: VIP blockade during neurogenesis induces microcephaly with thinner cortex.
A-B: Brain and body weight analyzes. VA injection in pregnant mice results in a selective reduction in brain weight of litters at P5 and P10 (1A, n=15 per group, unpaired t-test, * or #$p<0.05$) without significant body weight loss from controls (1B, n=15 per group, unpaired t-test, * or #$p<0.05$).
C-D: Coronal P5 brain sections labeled by Cresyl Violet staining shown at low (x2.5, 1A) and high (x10, 1B) magnifications, reveal a dramatic reduction in cortical surface and thickness in VA-treated animals when compared to age matched controls (Scale bars= 500 and 100µm, respectively).
E-G: At P5: quantification of cortical surface (C) and cortical thickness (D, E) in primary somatosensory cortex (S1) of Control and VA brains.
H: NeuN (F) immunostainings at high (x10) magnification. Note the proper lamination of the primary somatosensory cortex into six layers remains unchanged in VA as in control brains (Scale bars= 500µm).

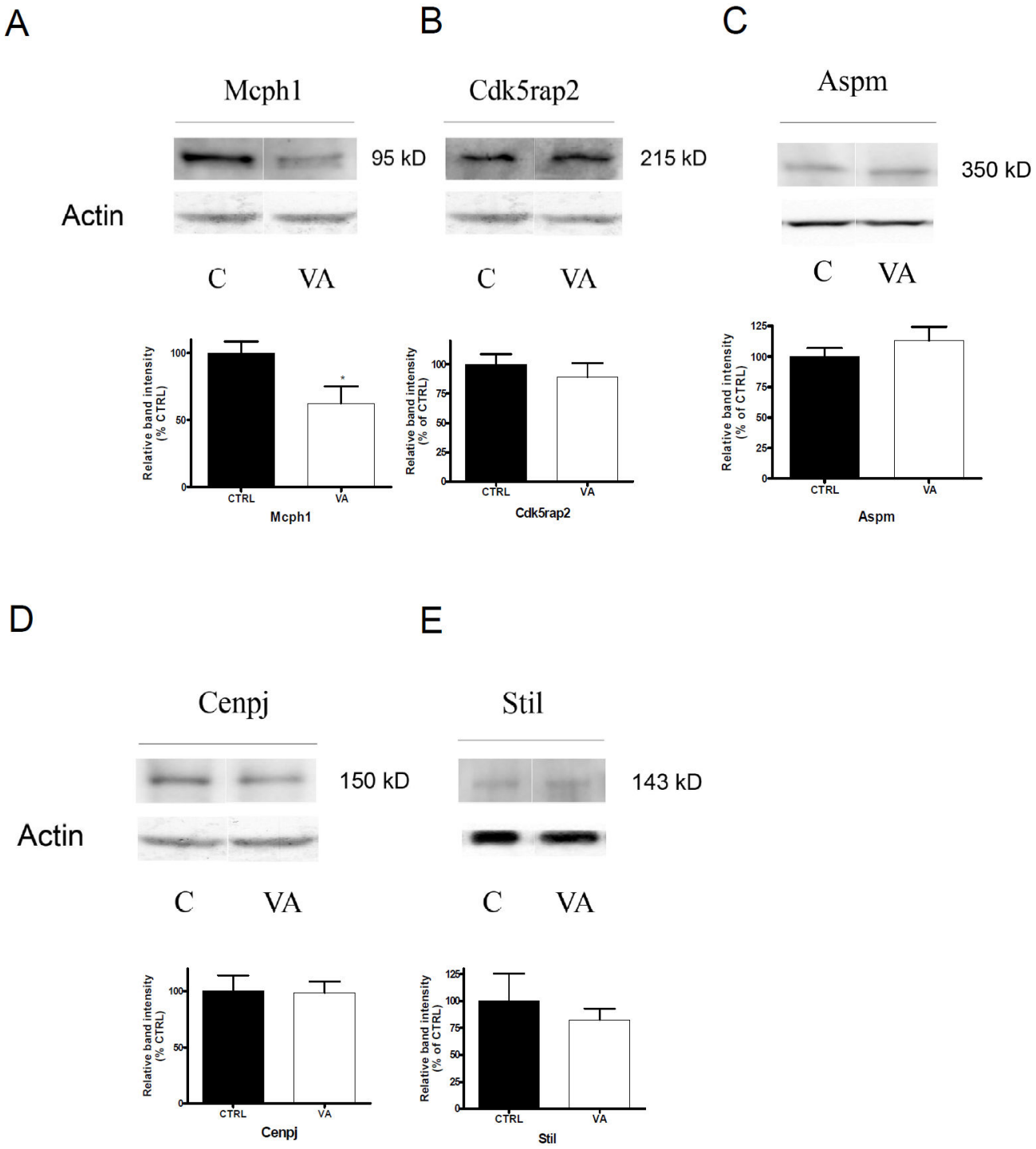

Supplemental Figure 2: VA treatment reduces the expression of Mcph1 protein at E12.5

A-E: Expression levels of Mcph1, Cdk5rap2, Aspm, Cenpj and Stil assessed by western blot on protein extracts from telencephalon of E12.5 embryos (CTRL or VA treated). Parallel to the reduction of *Mcph1* transcripts, VA induces a significant reduction in Mcph1 protein expression (n=8, t-test, $p<0.05$*) compared to CTRL at E12.5 (**A**). In contrast, no clear difference is observed between CTRL and VA extracts for Cdk5rap2, Aspm, Cenpj and Stil (**B-E**). The lanes were run on the same gel but were non-contiguous.

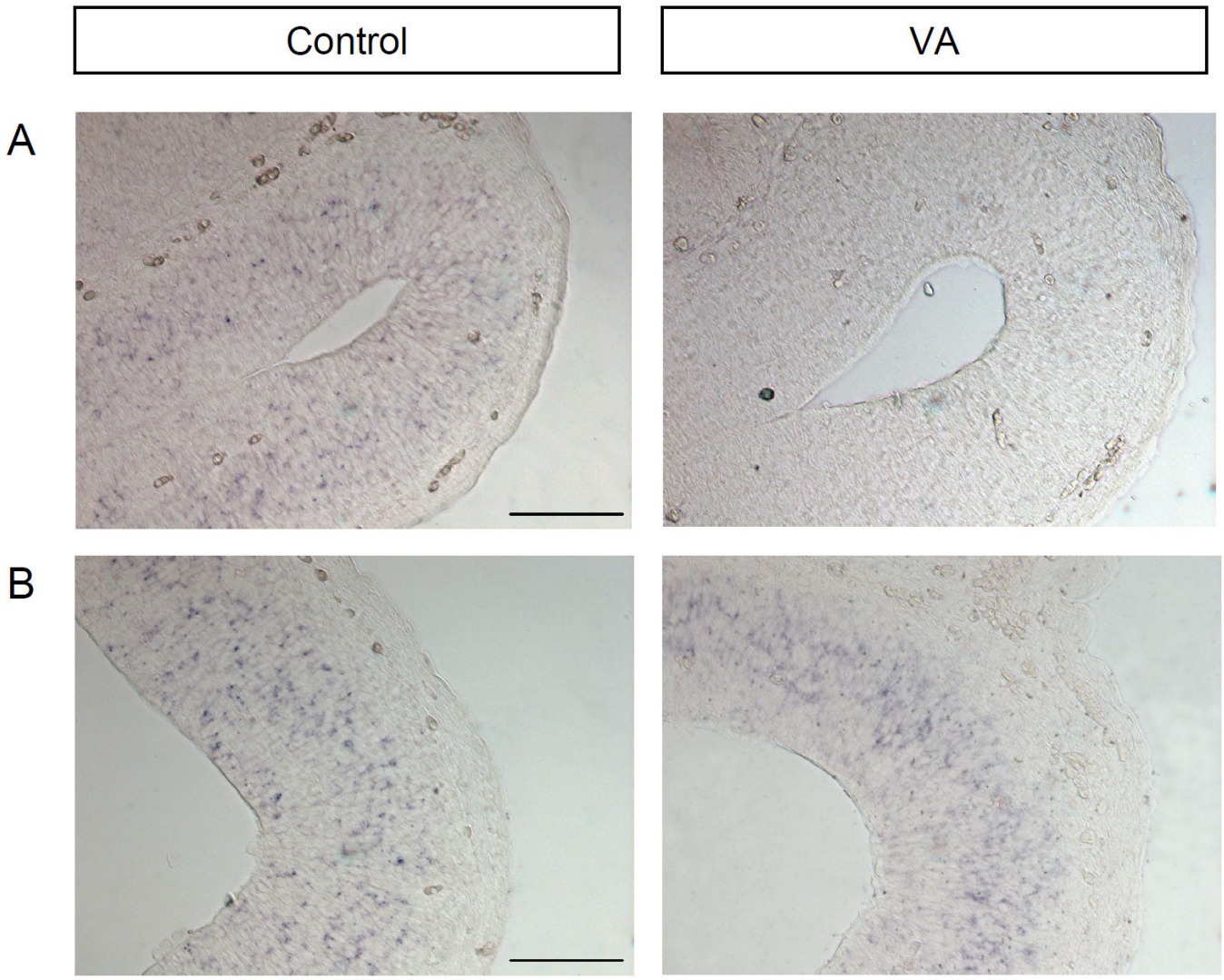

Supplemental Figure 3: VA treatment decreases the level of *Mcph1* expression and changes its pattern of expression

A-B: Expression of *Mcph1* gene by in situ hybridization in CTRL and VA treated embryos at E12. Expression of *Mcph1* gene is lost in the caudal area of the dorsal telencephalon of VA treated embryos when compared to CTRL at E12.5 (**A**). VA treatment changes the pattern of expression of *Mcph1* gene expression in the rostral area of the dorsal telencephalon relative to CTRL: *Mcph1* is not expressed in the neuroepithelium close to the ventricle when compared to CTRL (Scale bars= 40µm).

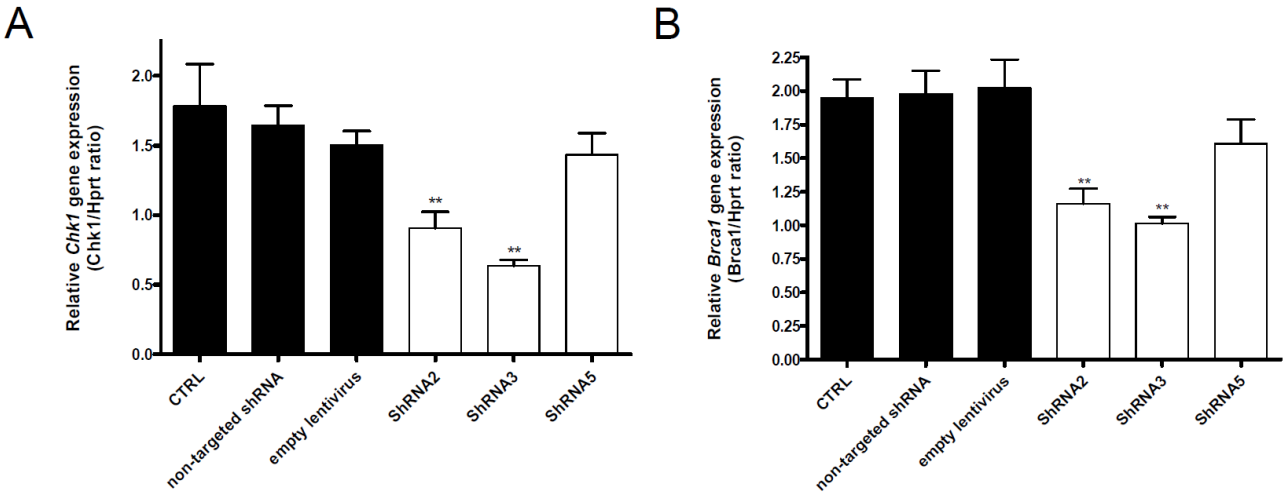

Supplemental Figure 4: Silencing of *Mcph1* gene expression reduces both *Chk1* and *Brca1* transcript levels
A-B: *Chk1* and *Brca1* expression levels assessed by quantitative RT-PCR on extracts from neurosphere-derived progenitors transduced by *Mcph1* specific lentiviral-mediated shRNA. Knock down of *Mcph1* expression by sequences shRNA 2 and 3 significantly reduces both *Chk1* and *Brca1* gene expression (n=3 per group, run in duplicate, one-way ANOVA, $p<0.05$*, $p<0.01$**, $p<0.001$***), while sequence shRNA5 failed to induce any significant silencing.

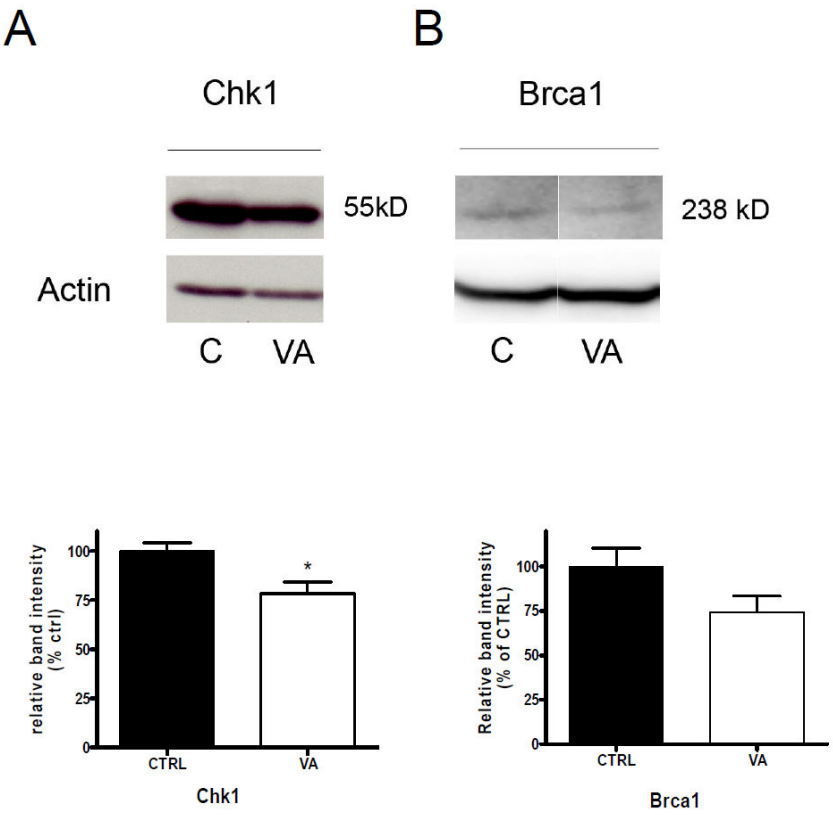

Supplemental Figure 5: VA treatment reduces Chk1 protein level at E12.5
A-B: Expression levels of Chk1 and Brca1 assessed by western blot on protein extracts from telencephalon of E12.5 embryos (CTRL or VA treated). Parallel to the reduction of *Chk1* transcripts, VA induces a significant reduction in Chk1 protein expression (n=8, t-test, $p<0.05$*) compared to CTRL at E12.5 (**A**) and, although not reaching statistical significance, a decrease of Brca1 protein expression (**B**). The lanes were run on the same gel but were non-contiguous.